

# Consistency of Functional Learning Methods Based on Derivatives

Fabrice Rossi<sup>a</sup>, Nathalie Villa-Vialaneix<sup>b,c,\*</sup>

<sup>a</sup>*Télécom ParisTech, LTCI - UMR CNRS 5141, France*

<sup>b</sup>*IUT de Perpignan (Dpt STID, Carcassonne), Université de Perpignan Via Domitia, France*

<sup>c</sup>*Institut de Mathématiques de Toulouse, Université de Toulouse, France*

---

## Abstract

In some real world applications, such as spectrometry, functional models achieve better predictive performances if they work on the derivatives of order  $m$  of their inputs rather than on the original functions. As a consequence, the use of derivatives is a common practice in functional data analysis, despite a lack of theoretical guarantees on the asymptotically achievable performances of a derivative based model. In this paper, we show that a smoothing spline approach can be used to preprocess multivariate observations obtained by sampling functions on a discrete and finite sampling grid in a way that leads to a consistent scheme on the original infinite dimensional functional problem. This work extends Mas and Pumo (2009) to nonparametric approaches and incomplete knowledge. To be more precise, the paper tackles two difficulties in a nonparametric framework: the information loss due to the use of the derivatives instead of the original functions and the information loss due to the fact that the functions are observed through a discrete sampling and are thus also unperfectly known: the use of a smoothing spline based approach solves these two problems. Finally, the proposed approach is tested on two real world datasets and the approach is experimentally proven to be a good solution in the case of noisy functional predictors.

**Keywords:** Functional Data Analysis, Consistency, Statistical learning, Derivatives, SVM, Smoothing splines, RKHS, Kernel

---

\*Corresponding author.

*Email addresses:* `Fabrice.Rossi@telecom-paristech.fr` (Fabrice Rossi), `nathalie.villa@math.univ-toulouse.fr` (Nathalie Villa-Vialaneix)

---

## 1. Introduction

As the measurement techniques are developping, more and more data are high dimensional vectors generated by measuring a continuous process on a discrete sampling grid. Many examples of this type of data can be found in real world applications, in various fields such as spectrometry, voice recognition, time series analysis, etc.

Data of this type should not be handled in the same way as standard multivariate observations but rather analysed as *functional* data: each observation is a function coming from an input space with infinite dimension, sampled on a high resolution sampling grid. This leads to a large number of variables, generally more than the number of observations. Moreover, functional data are frequently smooth and generate highly correlated variables as a consequence. Applied to the obtained high dimensional vectors, classical statistical methods (e.g., linear regression, factor analysis) often lead to ill-posed problems, especially when a covariance matrix has to be inverted (this is the case, e.g., in linear regression, in discriminant analysis and also in sliced inverse regression). Indeed, the number of observed values for each function is generally larger than the number of functions itself and these values are often strongly correlated. As a consequence, when these data are considered as multidimensional vectors, the covariance matrix is ill-conditioned and leads to unstable and unaccurate solutions in models where its inverse is required. Thus, these methods cannot be directly used. During past years, several methods have been adapted to that particular context and grouped under the generic name of Functional Data Analysis (FDA) methods. Seminal works focused on linear methods such as factorial analysis (Deville (1974); Dauxois and Pousse (1976); Besse and Ramsay (1986); James et al. (2000), among others) and linear models Ramsay and Dalzell (1991); Cardot et al. (1999); James and Hastie (2001); a comprehensive presentation of linear FDA methods is given in Ramsay and Silverman (1997, 2002). More recently, nonlinear functional models have been extensively developed and include generalized linear models James (2002); James and Silverman (2005), kernel nonparametric regression Ferraty and Vieu (2006), Functional Inverse Regression Ferré and Yao (2003), neural networks Rossi and Conan-Guez (2005); Rossi et al. (2005),  $k$ -nearest neighbors Biau et al. (2005); Laloë (2008), Support Vector Machines

36 (SVM), Rossi and Villa (2006), among a very large variety of methods.

37 In previous works, numerous authors have shown that the derivatives  
 38 of the functions lead sometimes to better predictive performances than the  
 39 functions themselves in inference tasks, as they provide information about  
 40 the shape or the regularity of the function. In particular applications such as  
 41 spectrometry Ferraty and Vieu (2006); Rossi et al. (2005); Rossi and Villa  
 42 (2006), micro-array data Dejean et al. (2007) and handwriting recognition  
 43 Williams et al. (2006); Bahlmann and Burkhardt (2004), these characteris-  
 44 tics lead to accurate predictive models. But, on a theoretical point of the  
 45 view, limited results about the effect of the use of the derivatives instead  
 46 of the original functions are available: Mas and Pumo (2009) studies this  
 47 problem for a linear model built on the first derivatives of the functions. In  
 48 the present paper, we also focus on the theoretical relevance of this common  
 49 practice and extend Mas and Pumo (2009) to nonparametric approaches and  
 50 incomplete knowledge.

51 More precisely, we address the problem of the estimation of the condi-  
 52 tional expectation  $\mathbb{E}(Y|X)$  of a random variable  $Y$  given a functional random  
 53 variable  $X$ .  $Y$  is assumed to be either real valued (leading to a regression  
 54 problem) or to take values in  $\{-1, 1\}$  (leading to a binary classification prob-  
 55 lem). We target two theoretical difficulties. The first difficulty is the potential  
 56 information loss induced by using a derivative instead of the original function:  
 57 when one replaces  $X$  by its order  $m$  derivative  $X^{(m)}$ , consistent estimators  
 58 (such as kernel models Ferraty and Vieu (2006)) guarantee an asymptotic  
 59 estimation of  $\mathbb{E}(Y|X^{(m)})$  but cannot be used directly to address the original  
 60 problem, namely estimating  $\mathbb{E}(Y|X)$ . This is a simple consequence of the  
 61 fact that  $X \mapsto X^{(m)}$  is not a one to one mapping. The second difficulty  
 62 is induced by sampling: in practice, functions are never observed exactly  
 63 but rather, as explained above, sampled on a discrete sampling grid. As a  
 64 consequence, one relies on approximate derivatives,  $\hat{X}_\tau^{(m)}$  (where  $\tau$  denotes  
 65 the sampling grid). This approach induces even more information loss with  
 66 respect to the underlying functional variable  $X$ : in general, a consistent es-  
 67 timator of  $\mathbb{E}(Y|\hat{X}_\tau^{(m)})$  will not provide a consistent estimation of  $\mathbb{E}(Y|X)$   
 68 and the optimal predictive performances for  $Y$  given  $\hat{X}_\tau^{(m)}$  will be lower than  
 69 the optimal predictive performances for  $Y$  given  $X$ .

70 We show in this paper that the use of a smoothing spline based approach  
 71 solves both problems. Smoothing splines are used to estimate the functions  
 72 from their sampled version in a convergent way. In addition, properties of

splines are used to obtain estimates of the derivatives of the functions with no induced information loss. Both aspects are implemented as a preprocessing step applied to the multivariate observations generated via the sampling grid. The preprocessed observations can then be fed into any finite dimensional consistent regression estimator or classifier, leading to a consistent estimator for the original infinite dimensional problem (in real world applications, we instantiate the general scheme in the particular case of kernel machines Shawe-Taylor and Cristianini (2004)).

The remainder of the paper is organized as follows: Section 2 introduces the model, the main smoothness assumption and the notations. Section 3 recalls important properties of spline smoothing. Section 4 presents approximation results used to build a general consistent classifier or a general consistent regression estimator in Section 5. Finally, Section 6 illustrates the behavior of the proposed method for two real world spectrometric problems. The proofs are given at the end of the article.

## 2. Setup and notations

### 2.1. Consistent classifiers and regression functions

We consider a pair of random variables  $(X, Y)$  where  $X$  takes values in a functional space  $\mathcal{X}$  and  $Y$  is either a real valued random variable (regression case) or a random variable taking values in  $\{-1, 1\}$  (binary classification case). From this, we are given a learning set  $S_n = \{(X_i, Y_i)\}_{i=1}^n$  of  $n$  independent copies of  $(X, Y)$ . Moreover, the functions  $X_i$  are not entirely known but sampled according to a non random sampling grid of finite length,  $\tau_d = (t_l)_{l=1}^{|\tau_d|}$ : we only observe  $\mathbf{X}_i^{\tau_d} = (X_i(t_1), \dots, X_i(t_{|\tau_d|}))^T$ , a vector of  $\mathbb{R}^{|\tau_d|}$  and denote  $S_{n, \tau_d}$  the corresponding learning set. Our goal is to construct:

1. *in the binary classification case*: a classifier,  $\phi_{n, \tau_d}$ , whose misclassification probability

$$L(\phi_{n, \tau_d}) = \mathbb{P}(\phi_{n, \tau_d}(\mathbf{X}^{\tau_d}) \neq Y)$$

asymptotically reaches the Bayes risk

$$L^* = \inf_{\phi: \mathcal{X} \rightarrow \{-1, 1\}} \mathbb{P}(\phi(X) \neq Y)$$

i.e.,  $\lim_{|\tau_d| \rightarrow +\infty} \lim_{n \rightarrow +\infty} \mathbb{E}(L(\phi_{n, \tau_d})) = L^*$  ;

102 2. *in the regression case*: a regression function,  $\phi_{n,\tau_d}$ , whose  $L^2$  error

$$L(\phi_{n,\tau_d}) = \mathbb{E}([\phi_{n,\tau_d}(\mathbf{X}^{\tau_d}) - Y]^2)$$

103 asymptotically reaches the minimal  $L^2$  error

$$L^* = \inf_{\phi: \mathcal{X} \rightarrow \mathbb{R}} \mathbb{E}([\phi(\mathbf{X}^{\tau_d}) - Y]^2)$$

104 i.e.,  $\lim_{|\tau_d| \rightarrow +\infty} \lim_{n \rightarrow +\infty} L(\phi_{n,\tau_d}) = L^*$ .

105 This definition implicitly requires  $\mathbb{E}(Y^2) < \infty$  and as a consequence,  
 106 corresponds to a  $L^2$  convergence of  $\phi_{n,\tau_d}$  to the conditional expectation  
 107  $\phi^* = \mathbb{E}(Y|X)$ , i.e., to  $\lim_{|\tau_d| \rightarrow +\infty} \lim_{n \rightarrow +\infty} \mathbb{E}([\phi_{n,\tau_d}(\mathbf{X}^{\tau_d}) - \phi^*(X)]^2) =$   
 108 0.

109 Such  $\phi_{n,\tau_d}$  are said to be (*weakly*) *consistent* Devroye et al. (1996);  
 110 Györfi et al. (2002). We have deliberately used the same notations for the  
 111 (optimal) predictive performances in both the binary classification and the  
 112 regression case. We will call  $L^*$  the Bayes risk even in the case of regression.  
 113 Most of the theoretical background of this paper is common to both the re-  
 114 gression case and the classification case: the distinction between both cases  
 115 will be made only when necessary.

116 As pointed out in the introduction, the main difficulty is to show that  
 117 the performances of a model built on the  $\mathbf{X}_i^{\tau_d}$  asymptotically reach the best  
 118 performance achievable on the original functions  $X_i$ . In addition, we will  
 119 build the model on derivatives estimated from the  $\mathbf{X}_i^{\tau_d}$ .

## 120 2.2. Smoothness assumption

121 Our goal is to leverage the functional nature of the data by allow-  
 122 ing differentiation operators to be applied to functions prior their submis-  
 123 sion to a more common classifier or regression function. Therefore we as-  
 124 sume that the functional space  $\mathcal{X}$  contains only differentiable functions.  
 125 More precisely,  $\mathcal{X}$  is the Sobolev space  $\mathcal{H}^m = \left\{ h \in L^2([0, 1]) \mid \forall j = \right.$   
 126  $1, \dots, m, D^j h \text{ exists in the weak sense, and } D^m h \in L^2([0, 1]) \left. \right\}$ , where  $D^j h$   
 127 is the  $j$ -th derivative of  $h$  (also denoted by  $h^{(j)}$ ) and for an integer  $m \geq 1$ .  
 128 Of course, by a straightforward generalization, any bounded interval can be  
 129 considered instead of  $[0, 1]$ .

130 To estimate the underlying functions  $X_i$  and their derivatives from sam-  
 131 pled data, we rely on smoothing splines. More precisely, let us consider  
 132 a deterministic function  $x \in \mathcal{H}^m$  sampled on the aforementioned grid. A  
 133 smoothing spline estimate of  $x$  is the solution,  $\hat{x}_{\lambda, \tau_d}$ , of

$$\arg \min_{h \in \mathcal{H}^m} \frac{1}{|\tau_d|} \sum_{l=1}^{|\tau_d|} (x(t_l) - h(t_l))^2 + \lambda \int_{[0,1]} (h^{(m)}(t))^2 dt, \quad (1)$$

134 where  $\lambda$  is a regularization parameter that balances interpolation error and  
 135 smoothness (measured by the  $L^2$  norm of the  $m$ -th derivative of the esti-  
 136 mate). The goal is to show that a classifier or a regression function built  
 137 on  $\hat{X}_{\lambda, \tau_d}^{(m)}$  is consistent for the original problem (i.e., the problem defined by  
 138 the pair  $(X, Y)$ ): this means that using  $\hat{X}_{\lambda, \tau_d}^{(m)}$  instead of  $X$  has no dramatic  
 139 consequences on the accuracy of the classifier or of the regression function.  
 140 In other words, asymptotically, no information loss occurs when one replaces  
 141  $X$  by  $\hat{X}_{\lambda, \tau_d}^{(m)}$ .

142 The proof is based on the following steps:

- 143 1. First, we show that building a classifier or a regression function on  
 144  $\hat{X}_{\lambda, \tau_d}^{(m)}$  is approximately equivalent to building a classifier or a regression  
 145 function on  $\mathbf{X}^{\tau_d} = (X(t_l))_{l=1}^{|\tau_d|}$  using a specific metric. This is done by  
 146 leveraging the Reproducing Kernel Hilbert Space (RKHS) structure of  
 147  $\mathcal{H}^m$ . This part serves one main purpose: it provides a solution to work  
 148 with estimation of the derivatives of the original function in a way  
 149 that preserves all the information available in  $\mathbf{X}^{\tau_d}$ . In other words, the  
 150 best predictive performances for  $Y$  theoretically available by building a  
 151 multivariate model on  $\mathbf{X}^{\tau_d}$  are equal to the best predictive performances  
 152 obtained by building a functional model on  $\hat{X}_{\lambda, \tau_d}^{(m)}$ .
- 153 2. Then, we link  $\mathbb{E}(Y|\hat{X}_{\lambda, \tau_d})$  with  $\mathbb{E}(Y|X)$  by approximation results  
 154 available for smoothing splines. This part of the proof handles the  
 155 effects of sampling.
- 156 3. Finally, we glue both results via standard  $\mathbb{R}^{|\tau_d|}$  consistency results.

### 157 3. Smoothing splines and differentiation operators

#### 158 3.1. RKHS and smoothing splines

159 As we want to work on derivatives of functions from  $\mathcal{H}^m$ , a natural in-  
 160 ner product for two functions of  $\mathcal{H}^m$  would be  $(u, v) \rightarrow \int_0^1 u^{(m)}(t)v^{(m)}(t)dt$ .  
 161 However, we prefer to use an inner product of  $\mathcal{H}^m$  ( $\int_0^1 u^{(m)}(t)v^{(m)}(t)dt$  only  
 162 induces a semi-norm on  $\mathcal{H}^m$ ) because, as will be shown later, such an in-  
 163 ner product is related to an inner product between the sampled functions  
 164 considered as vectors of  $\mathbb{R}^{|\tau_d|}$ .

165 This can be done by decomposing  $\mathcal{H}^m$  into  $\mathcal{H}^m = \mathcal{H}_0^m \oplus \mathcal{H}_1^m$   
 166 Kimeldorf and Wahba (1971), where  $\mathcal{H}_0^m = \text{Ker} D^m = \mathbb{P}^{m-1}$  (the space of  
 167 polynomial functions of degree less or equal to  $m-1$ ) and  $\mathcal{H}_1^m$  is an infi-  
 168 nite dimensional subspace of  $\mathcal{H}^m$  defined via  $m$  boundary conditions. The  
 169 boundary conditions are given by a full rank linear operator from  $\mathcal{H}^m$  to  $\mathbb{R}^m$ ,  
 170 denoted  $B$ , such that  $\text{Ker} B \cap \mathbb{P}^{m-1} = \{0\}$ . Classical examples of boundary  
 171 conditions include the case of “natural splines” (for  $m=2$ ,  $h(0)=h(1)=0$ )  
 172 and constraints that target only the first values of  $h$  and its derivatives at  
 173 a fixed position, for instance the conditions:  $h(0) = \dots = h^{(m-1)}(0) = 0$ .  
 174 Other boundary conditions can be used Berlinet and Thomas-Agnan (2004);  
 175 Besse and Ramsay (1986); Craven and Wahba (1978), depending on the ap-  
 176 plication.

177 Once the boundary conditions are fixed, an inner product on both  $\mathcal{H}_0^m$   
 178 and  $\mathcal{H}_1^m$  can be defined:

$$\langle u, v \rangle_1 = \langle D^m u, D^m v \rangle_{L^2} = \int_0^1 u^{(m)}(t)v^{(m)}(t)dt$$

179 is an inner product on  $\mathcal{H}_1^m$  (as  $h \in \mathcal{H}_1^m$  and  $D^m h \equiv 0$  give  $h \equiv 0$ ). Moreover,  
 180 if we denote  $B = (B^j)_{j=1}^m$ , then  $\langle u, v \rangle_0 = \sum_{j=1}^m B^j u B^j v$  is an inner product  
 181 on  $\mathcal{H}_0^m$ . We obtain this way an inner product on  $\mathcal{H}^m$  given by

$$\begin{aligned} \langle u, v \rangle_{\mathcal{H}^m} &= \int_0^1 u^{(m)}(t)v^{(m)}(t)dt + \sum_{j=1}^m B^j u B^j v \\ &= \langle \mathcal{P}_1^m(u), \mathcal{P}_1^m(v) \rangle_1 + \langle \mathcal{P}_0^m(u), \mathcal{P}_0^m(v) \rangle_0 \end{aligned}$$

182 where  $\mathcal{P}_i^m$  is the projector on  $\mathcal{H}_i^m$ .

183 Equipped with  $\langle \cdot, \cdot \rangle_{\mathcal{H}^m}$ ,  $\mathcal{H}^m$  is a Reproducing Kernel Hilbert Space  
 184 (RKHS, see e.g. Berlinet and Thomas-Agnan (2004); Heckman and Ramsay

(2000); Wahba (1990)). More precisely, it exists a kernel  $k : [0, 1]^2 \rightarrow \mathbb{R}$  such that, for all  $u \in \mathcal{H}^m$  and all  $t \in [0, 1]$ ,  $\langle u, k(t, \cdot) \rangle_{\mathcal{H}^m} = u(t)$ . The same occurs for  $\mathcal{H}_0^m$  and  $\mathcal{H}_1^m$  which respectively have reproducing kernels denoted by  $k_0$  and  $k_1$ . We have  $k = k_0 + k_1$ .

In the most common cases,  $k_0$  and  $k_1$  have already been explicitly calculated (see e.g., Berlinet and Thomas-Agnan (2004), especially chapter 6, sections 1.1 and 1.6.2). For example, for  $m \geq 1$  and the boundary conditions  $h(0) = h'(0) = \dots = h^{(m-1)}(0) = 0$ , we have:

$$k_0(s, t) = \sum_{k=0}^{m-1} \frac{t^k s^k}{(k!)^2}.$$

and

$$k_1(s, t) = \int_0^1 \frac{(t-w)_+^{m-1} (s-w)_+^{m-1}}{(m-1)!^2} dw.$$

### 3.2. Computing the splines

We need now to compute to  $\hat{x}_{\lambda, \tau_d}$  starting with  $\mathbf{x}^{\tau_d} = (x(t))_{t \in \tau_d}^T$ . This can be done via a theorem from Kimeldorf and Wahba (1971). We need the following compatibility assumptions between the sampling grid  $\tau_d$  and the boundary conditions operator  $B$ :

**Assumption 1.** *The sampling grid  $\tau_d = (t_l)_{l=1}^{|\tau_d|}$  is such that*

1. *sampling points are distinct in  $[0, 1]$  and  $|\tau_d| \geq m - 1$*
2. *the  $m$  boundary conditions  $B^j$  are linearly independent from the  $|\tau_d|$  linear forms  $h \mapsto h(t_l)$ , for  $l = 1, \dots, |\tau_d|$  (defined on  $\mathcal{H}^m$ )*

Then  $\hat{x}_{\lambda, \tau_d}$  and  $\mathbf{x}^{\tau_d} = (x(t))_{t \in \tau_d}^T$  are linked by the following result:

**Theorem 1** (Kimeldorf and Wahba (1971)). *Under Assumption (A1), the unique solution  $\hat{x}_{\lambda, \tau_d}$  to equation (1) is given by:*

$$\hat{x}_{\lambda, \tau_d} = \mathcal{S}_{\lambda, \tau_d} \mathbf{x}^{\tau_d}, \quad (2)$$

where  $\mathcal{S}_{\lambda, \tau_d}$  is a full rank linear operator from  $\mathbb{R}^{|\tau_d|}$  to  $\mathcal{H}^m$  defined by:

$$\mathcal{S}_{\lambda, \tau_d} = \omega^T M_0 + \eta^T M_1 \quad (3)$$

with



- 208 •  $M_0 = (U(K_1 + \lambda I_d)^{-1} U^T)^{-1} U(K_1 + \lambda I_d)^{-1}$
- 209 •  $M_1 = (K_1 + \lambda I_d)^{-1} (I_d - U^T M_0)$ ;
- 210 •  $\{\omega_1, \dots, \omega_m\}$  is a basis of  $\mathbb{P}^{m-1}$ ,  $\omega = (\omega_1, \dots, \omega_m)^T$  and  $U =$
- 211  $(\omega_i(t))_{i=1, \dots, m}^T$   $t \in \tau_d$ ;
- 212 •  $\eta = (k_1(t, \cdot))_{t \in \tau_d}^T$  and  $K_1 = (k_1(t, t'))_{t, t' \in \tau_d}$ .

### 213 3.3. No information loss

214 The first important consequence of Theorem 1 is that building a model  
 215 on  $\hat{X}_{\lambda, \tau_d}$  or on  $\mathbf{X}^{\tau_d}$  leads to the same optimal predictive performances (to the  
 216 same Bayes risk). This is formalized by the following corollary:

217 **Corollary 1.** *Under Assumption (A1), we have*

- 218 • *in the binary classification case:*

$$\inf_{\phi: \mathcal{H}^m \rightarrow \{-1, 1\}} \mathbb{P}(\phi(\hat{X}_{\lambda, \tau_d}) \neq Y) = \inf_{\phi: \mathbb{R}^{|\tau_d|} \rightarrow \{-1, 1\}} \mathbb{P}(\phi(\mathbf{X}^{\tau_d}) \neq Y) \quad (4)$$

- 219 • *in the regression case:*

$$\inf_{\phi: \mathcal{H}^m \rightarrow \mathbb{R}} \mathbb{E} \left( \left[ \phi(\hat{X}_{\lambda, \tau_d}) - Y \right]^2 \right) = \inf_{\phi: \mathbb{R}^{|\tau_d|} \rightarrow \mathbb{R}} \mathbb{E} ([\phi(\mathbf{X}^{\tau_d}) - Y]^2) \quad (5)$$

### 220 3.4. Differentiation operator

221 The second important consequence of Theorem 1 is that the inner product  
 222  $\langle \cdot, \cdot \rangle_{\mathcal{H}^m}$  is equivalent to a specific inner product on  $\mathbb{R}^{|\tau_d|}$  given in the following  
 223 corollary:

224 **Corollary 2.** *Under Assumption (A1) and for any  $\mathbf{u}^{\tau_d} = (u(t))_{t \in \tau_d}^T$  and*  
 225  $\mathbf{v}^{\tau_d} = (v(t))_{t \in \tau_d}^T$  *in  $\mathbb{R}^{|\tau_d|}$ ,*

$$\langle \hat{u}_{\lambda, \tau_d}, \hat{v}_{\lambda, \tau_d} \rangle_{\mathcal{H}^m} = (\mathbf{u}^{\tau_d})^T \mathbf{M}_{\lambda, \tau_d} \mathbf{v}^{\tau_d} \quad (6)$$

226 where  $\mathbf{M}_{\lambda, \tau_d} = M_0^T W M_0 + M_1^T K_1 M_1$  with  $W = (\langle w_i, w_j \rangle_0)_{i, j=1, \dots, m}$ . The  
 227 matrix  $\mathbf{M}_{\lambda, \tau_d}$  is symmetric and positive definite and defines an inner product  
 228 on  $\mathbb{R}^{|\tau_d|}$ .

229 The corollary is a direct consequence of equations (2) and (3).

230 In practice, the corollary means that the euclidean space  $(\mathbb{R}^{|\tau_d|}, \langle \cdot, \cdot \rangle_{\mathbf{M}_{\lambda, \tau_d}})$   
 231 is isomorphic to  $(\mathcal{I}_{\lambda, \tau_d}, \langle \cdot, \cdot \rangle_{\mathcal{H}^m})$ , where  $\mathcal{I}_{\lambda, \tau_d}$  is the image of  $\mathbb{R}^{|\tau_d|}$  by  $\mathcal{S}_{\lambda, \tau_d}$ . As  
 232 a consequence, one can use the Hilbert structure of  $\mathcal{H}^m$  directly in  $\mathbb{R}^{|\tau_d|}$  via  
 233  $\mathbf{M}_{\lambda, \tau_d}$ : as the inner product of  $\mathcal{H}^m$  is defined on the order  $m$  derivatives of the  
 234 functions, this corresponds to using those derivatives instead of the original  
 235 functions.

236 More precisely, let  $\mathbf{Q}_{\lambda, \tau_d}$  be the transpose of the Cholesky triangle of  $\mathbf{M}_{\lambda, \tau_d}$   
 237 (given by the Cholesky decomposition  $\mathbf{Q}_{\lambda, \tau_d}^T \mathbf{Q}_{\lambda, \tau_d} = \mathbf{M}_{\lambda, \tau_d}$ ). Corollary 2  
 238 shows that  $\mathbf{Q}_{\lambda, \tau_d}$  acts as an approximate differentiation operation on sampled  
 239 functions.

240 Let us indeed consider an estimation method for multivariate inputs based  
 241 only on inner products or norms (that are directly derived from the in-  
 242 ner products), such as, e.g., Kernel Ridge Regression Saunders et al. (1998);  
 243 Shawe-Taylor and Cristianini (2004). In this latter case, if a Gaussian kernel  
 244 is used, the regression function has the following form:

$$u \mapsto \sum_{i=1}^n T_i \alpha_i e^{-\gamma \|U_i - u\|_{\mathbb{R}^p}^2} \quad (7)$$

245 where  $(U_i, T_i)_{1 \leq i \leq n}$  are learning examples in  $\mathbb{R}^p \times \{-1, 1\}$  and the  $\alpha_i$  are non  
 246 negative real values obtained by solving a quadratic programming problem  
 247 and  $\gamma$  is a parameter of the method. Then, if we use Kernel Ridge Regression  
 248 on the training set  $\{(\mathbf{Q}_{\lambda, \tau_d} \mathbf{X}_i^{\tau_d}, Y_i)\}_{i=1}^n$  (rather than the original training set  
 249  $\{(\mathbf{X}_i^{\tau_d}, Y_i)\}_{i=1}^n$ ), it will work on the norm in  $L^2$  of the derivatives of order  
 250  $m$  of the spline estimates of the  $X_i$  (up to the boundary conditions). More  
 251 precisely, the regression function will have the following form:

$$\begin{aligned} \mathbf{x}^{\tau_d} &\mapsto \sum_{i=1}^n Y_i \alpha_i e^{-\gamma \|\mathbf{Q}_{\lambda, \tau_d} \mathbf{X}_i^{\tau_d} - \mathbf{Q}_{\lambda, \tau_d} \mathbf{x}^{\tau_d}\|_{\mathbb{R}^{|\tau_d|}}^2} \\ &\mapsto \sum_{i=1}^n Y_i \alpha_i e^{-\gamma \|D^m \widehat{X}_{i, \lambda, \tau_d} - D^m \widehat{x}_{\lambda, \tau_d}\|_{L^2}^2} \\ &\quad \times e^{-\gamma \sum_{j=1}^m (B^j \widehat{X}_{i, \lambda, \tau_d} - B^j \widehat{x}_{\lambda, \tau_d})^2} \end{aligned}$$

252 In other words, up to the boundary conditions, an estimation method based  
 253 solely on inner products, or on norms derived from these inner products,

can be given modified inputs that will make it work on an estimation of the derivatives of the observed functions.

**Remark 1.** As shown in Corollary 1 in the previous section, building a model on  $\mathbf{X}^{\tau_d}$  or on  $\hat{X}_{\lambda, \tau_d}$  leads to the same optimal predictive performances. In addition, it is obvious that given any one-to-one mapping  $f$  from  $\mathbb{R}^{|\tau_d|}$  to itself, building a model on  $f(\mathbf{X}^{\tau_d})$  gives also the same optimal performances than building a model on  $\mathbf{X}^{\tau_d}$ . Then as  $\mathbf{Q}_{\lambda, \tau_d}$  is invertible, the optimal predictive performances achievable with  $\mathbf{Q}_{\lambda, \tau_d} \mathbf{X}^{\tau_d}$  are equal to the optimal performances achievable with  $\mathbf{X}^{\tau_d}$  or with  $\hat{X}_{\lambda, \tau_d}$ .

In practice however, the actual preprocessing of the data can have a strong influence on the obtained performances, as will be illustrated in Section 6. The goal of the theoretical analysis of the present section is to guarantee that no systematic loss can be observed as a consequence of the proposed functional preprocessing scheme.

#### 4. Approximation results

The previous section showed that working on  $\mathbf{X}^{\tau_d}$ ,  $\mathbf{Q}_{\lambda, \tau_d} \mathbf{X}^{\tau_d}$  or  $\hat{X}_{\lambda, \tau_d}$  makes no difference in terms of optimal predictive performances. The present section addresses the effects of sampling: asymptotically, the optimal predictive performances obtained on  $\hat{X}_{\lambda, \tau_d}$  converge to the optimal performances achievable on the original and unobserved functional variable  $X$ .

##### 4.1. Spline approximation

From the sampled random function  $\mathbf{X}^{\tau_d} = (X(t_1), \dots, X(t_{|\tau_d|}))$ , we can build an estimate,  $\hat{X}_{\lambda, \tau_d}$ , of  $X$ . To ensure consistency, we must guarantee that  $\hat{X}_{\lambda, \tau_d}$  converges to  $X$ . In the case of a deterministic function  $x$ , this problem has been studied in numerous papers, such as Craven and Wahba (1978); Ragozin (1983); Cox (1984); Utreras (1988); Wahba (1990) (among others). Here we recall one of the results which is particularly well adapted to our context.

Obviously, the sampling grid must behave correctly, whereas the information contained in  $\mathbf{X}^{\tau_d}$  will not be sufficient to recover  $X$ . We need also the regularization parameter  $\lambda$  to depend on  $\tau_d$ . Following Ragozin (1983), a sampling grid  $\tau_d$  is characterized by two quantities:

$$\begin{aligned} \overline{\Delta}_{\tau_d} &= \max\{t_1, t_2 - t_1, \dots, 1 - t_{|\tau_d|}\} \\ \underline{\Delta}_{\tau_d} &= \min_{1 \leq i < |\tau_d|} \{t_{i+1} - t_i\}. \end{aligned} \tag{8}$$

One way to control the distance between  $X$  and  $\hat{X}_{\lambda, \tau_d}$  is to bound the ratio  $\bar{\Delta}_{\tau_d}/\underline{\Delta}_{\tau_d}$  so as to ensure quasi-uniformity of the sampling grid.

More precisely, we will use the following assumption:

**Assumption 2.** *There is  $R$  such that  $\bar{\Delta}_{\tau_d}/\underline{\Delta}_{\tau_d} \leq R$  for all  $d$ .*

Then we have:

**Theorem 2** (Ragozin (1983)). *Under Assumptions (A1) and (A2), there are two constants  $A_{R,m}$  and  $B_{R,m}$  depending only on  $R$  and  $m$ , such that for any  $x \in \mathcal{H}^m$  and any positive  $\lambda$ :*

$$\|\hat{x}_{\lambda, \tau_d} - x\|_{L^2}^2 \leq \left( A_{R,m} \lambda + B_{R,m} \frac{1}{|\tau_d|^{2m}} \right) \|D^m x\|_{L^2}^2.$$

This result is a rephrasing of Corollary 4.16 from Ragozin (1983) which is itself a direct consequence of Theorem 4.10 from the same paper.

Convergence of  $\hat{x}_{\lambda, \tau_d}$  to  $x$  is then obtained by the following simple assumptions:

**Assumption 3.** *The series of sampling points  $\tau_d$  and the series of regularization parameters,  $\lambda$ , depending on  $\tau_d$  and denoted by  $(\lambda_d)_{d \geq 1}$ , are such that  $\lim_{d \rightarrow +\infty} |\tau_d| = +\infty$  and  $\lim_{d \rightarrow +\infty} \lambda_d = 0$ .*

#### 4.2. Conditional expectation approximation

The next step consists in relating the optimal predictive performances for the regression and the classification problem  $(X, Y)$  to the performances associated to  $(\hat{X}_{\lambda_d, \tau_d}, Y)$  when  $d$  goes to infinity, i.e., relating  $L^*$  to

1. *binary classification case:*

$$L_d^* = \inf_{\phi: \mathcal{H}^m \rightarrow \{-1, 1\}} \mathbb{P} \left( \phi(\hat{X}_{\lambda_d, \tau_d}) \neq Y \right),$$

2. *regression case:*

$$L_d^* = \inf_{\phi: \mathcal{H}^m \rightarrow \mathbb{R}} \mathbb{E} \left( [\phi(\hat{X}_{\lambda_d, \tau_d}) - Y]^2 \right)$$

Two sets of assumptions will be investigated to provide the convergence of the Bayes risk  $L_d^*$  to  $L^*$ :

309 **Assumption 4. Either**

310 (A4a)  $\mathbb{E}(\|D^m X\|_{L^2}^2)$  is finite and  $Y \in \{-1, 1\}$ ,

311 **or**

312 (A4b)  $\tau_d \subset \tau_{d+1}$  and  $\mathbb{E}(Y^2)$  is finite.

313 The first assumption (A4a) requires an additional smoothing property for  
 314 the predictor functional variable  $X$  and is only valid for a binary classifica-  
 315 tion problem whereas the second assumption (A4a) requires an additional  
 316 property for the sampling point series: they have to be growing sets.

317 Theorem 2 then leads to the following corollary:

318 **Corollary 3.** *Under Assumptions (A1)-(A4), we have:*

$$\lim_{d \rightarrow +\infty} L_d^* = L^*.$$

319 **5. General consistent functional classifiers and regression functions**

320 *5.1. Definition of classifiers and regression functions on derivatives*

321 Let us now consider any consistent classification or regression scheme  
 322 for standard multivariate data based either on the inner product or on  
 323 the Euclidean distance between observations. Examples of such classifiers  
 324 are Support Vector Machine Steinwart (2002), the kernel classification rule  
 325 Devroye and Krzyżak (1989) and  $k$ -nearest neighbors Devroye and Györfi  
 326 (1985); Zhao (1987) to name a few. In the same way, multilayer perceptrons  
 327 Lugosi and Zeger (1990), kernel estimates Devroye and Krzyżak (1989) and  
 328  $k$ -nearest neighbors regression Devroye et al. (1994) are consistent regression  
 329 estimators. Additional examples of consistent estimators in classification and  
 330 regression can be found in Devroye et al. (1996); Györfi et al. (2002).

331 We denote  $\psi_{\mathcal{D}}$  the estimator constructed by the chosen scheme using a  
 332 dataset  $\mathcal{D} = \{(U_i, T_i)_{1 \leq i \leq n}\}$ , where the  $(U_i, T_i)_{1 \leq i \leq n}$  are  $n$  independent copies  
 333 of a pair of random variables  $(U, T)$  with values in  $\mathbb{R}^p \times \{-1, 1\}$  (classification)  
 334 or  $\mathbb{R}^p \times \mathbb{R}$  (regression).

335 The proposed functional scheme consists in choosing the estimator  $\phi_{n, \tau_d}$   
 336 as  $\psi_{\mathcal{E}_{n, \tau_d}}$  with the dataset  $\mathcal{E}_{n, \tau_d}$  defined by:

$$\mathcal{E}_{n, \tau_d} = \{(\mathbf{Q}_{\lambda_d, \tau_d} \mathbf{X}_i^{\tau_d}, Y_i)_{1 \leq i \leq n}\}$$

337 As pointed out in Section 3.4, the linear transformation  $\mathbf{Q}_{\lambda_d, \tau_d}$  is an approx-  
 338 imate multivariate differentiation operator: up to the boundary conditions,  
 339 an estimator based on  $\mathbf{Q}_{\lambda_d, \tau_d} \mathbf{X}^{\tau_d}$  is working on the  $m$ -th derivative of  $\widehat{X}_{\lambda_d, \tau_d}$ .

340 In more algorithmic terms, the estimator is obtained as follows:

- 341 1. choose an appropriate value for  $\lambda_d$
- 342 2. compute  $\mathbf{M}_{\lambda_d, \tau_d}$  using Theorem 1 and Corollary 2;
- 343 3. compute the Cholesky decomposition of  $\mathbf{M}_{\lambda_d, \tau_d}$  and the transpose of  
 344 the Cholesky triangle,  $\mathbf{Q}_{\lambda_d, \tau_d}$  (such that  $\mathbf{Q}_{\lambda_d, \tau_d}^T \mathbf{Q}_{\lambda_d, \tau_d} = \mathbf{M}_{\lambda_d, \tau_d}$ );
- 345 4. compute  $\mathbf{Q}_{\lambda_d, \tau_d} \mathbf{X}_i^{\tau_d}$  to obtain the transformed dataset  $\mathcal{E}_{n, \tau_d}$ ;
- 346 5. build a classifier/regression function  $\psi_{\mathcal{E}_{n, \tau_d}}$  with a multivariate method  
 347 in  $\mathbb{R}^{|\tau_d|}$  applied to the dataset  $\mathcal{E}_{n, \tau_d}$ ;
- 348 6. associate to a new sampled function  $\mathbf{X}_{n+1}^{\tau_d}$  the prediction  
 349  $\psi_{\mathcal{E}_{n, \tau_d}}(\mathbf{Q}_{\lambda, \tau_d} \mathbf{X}_{n+1}^{\tau_d})$ .

350 Figure 5.1 illustrates the way the method performs: instead of relying  
 351 on an approximation of the function and then on the derivation preprocess-  
 352 ing of this estimates, it directly uses an equivalent metric by applying the  
 353  $\mathbf{Q}_{\lambda_d, \tau_d}$  matrix to the sampled function. The consistency result proved in The-  
 354 orem 3 shows that, combined with any consistent multidimensional learning  
 355 algorithm, this method is (asymptotically) equivalent to using the original  
 356 function drawn at the top left side of Figure 5.1.

357 On a practical point of view, Wahba (1990) demonstrates that cross val-  
 358 idated estimates of  $\lambda$  achieve suitable convergence rates. Hence, steps 1 and  
 359 2 can be computed simultaneously by minimizing the total cross validated  
 360 error for all the observations, given by

$$\sum_{i=1}^n \frac{1}{|\tau_d|} \sum_{t \in \tau_d} \frac{(x_i(t) - \widehat{x}_{i, \lambda, \tau_d}(t))^2}{(1 - A_{tt}(\lambda))^2},$$

361 where  $A$  is a  $|\tau_d| \times |\tau_d|$  matrix called the *influence matrix* (see Wahba (1990)),  
 362 over a finite number of  $\lambda$  values.

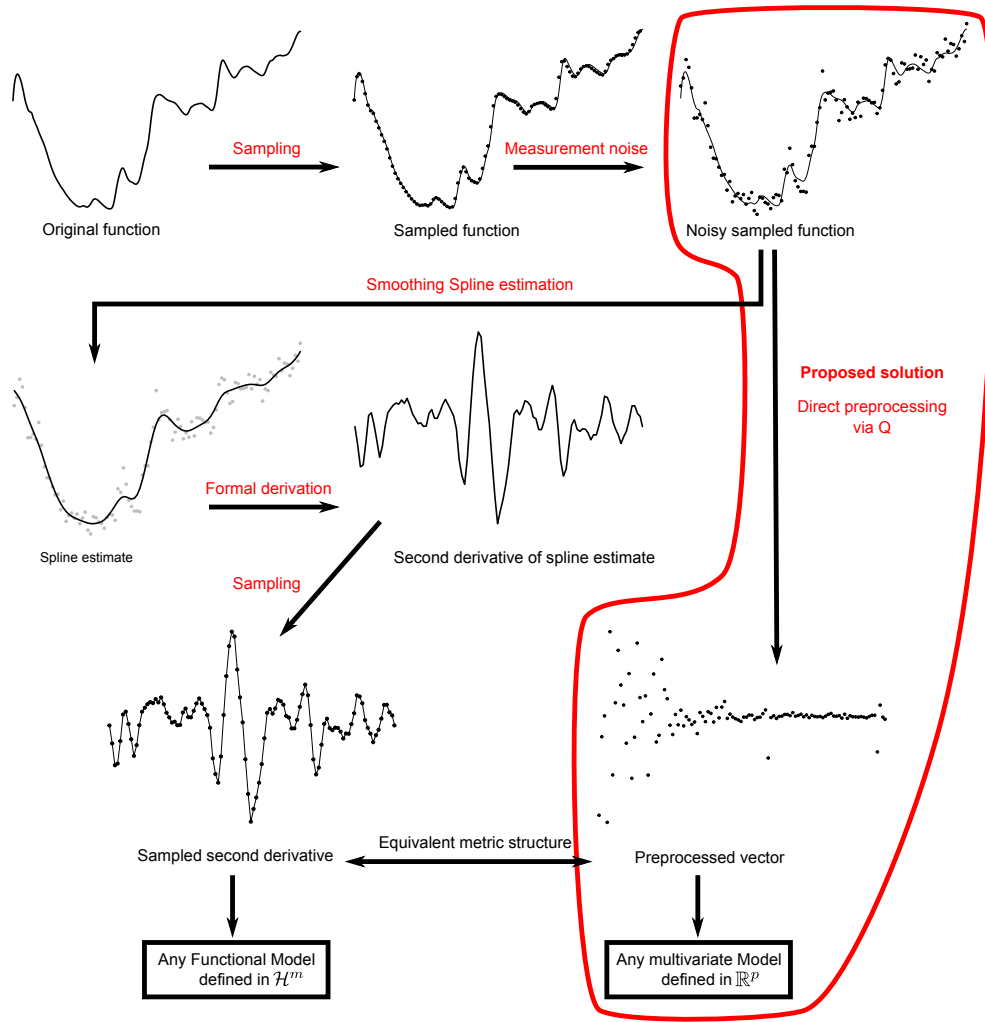


Figure 1: Method scheme and its equivalence to the usual approach for using derivatives in learning algorithms.

### 363 5.2. Consistency result

364 Corollary 1 and Corollary 3 guarantee that the estimator proposed in the  
365 previous section is consistent:

366 **Theorem 3.** *Under assumptions (A1)-(A4), the series of classi-*  
367 *fiers/regression functions  $(\phi_{n,\tau_d})_{n,d}$  is consistent:*

$$\lim_{d \rightarrow +\infty} \lim_{n \rightarrow +\infty} \mathbb{E} (L\phi_{n,\tau_d}) = L^*$$

### 368 5.3. Discussion

369 While Theorem 3 is very general, it could be easily extended to cover  
370 special cases such as additional hypothesis needed by the estimation scheme  
371 or to provide data based parameter selections. We discuss briefly those issues  
372 in the present section.

373 It should first be noted that most estimation schemes,  $\psi_{\mathcal{D}}$ , depend on  
374 parameters that should fulfill some assumptions for the scheme to be con-  
375 sistent. For instance, in the Kernel Ridge Regression method in  $\mathbb{R}^p$ , with  
376 Gaussian kernel,  $\psi_{\mathcal{D}}$  has the form given in Equation (7) where the  $(\alpha_i)$  are  
377 the solutions of

$$\begin{aligned} \arg \min_{\alpha \in \mathbb{R}^n} \sum_{i=1}^n \left( T_i - \sum_{j=1}^n T_j \alpha_j e^{-\gamma \|U_i - U_j\|_{\mathbb{R}^p}^2} \right)^2 + \\ \delta_n \sum_{i,j=1}^n T_i T_j \alpha_i \alpha_j e^{-\gamma \|U_i - U_j\|_{\mathbb{R}^p}^2}. \end{aligned}$$

378 The method thus depends on the parameter of the Gaussian kernel,  $\gamma$  and  
379 of the regularization parameter  $\delta_n$ . This method is known to be consistent if  
380 (see Theorem 9.1 of Steinwart and Christmann (2008)):

$$\delta_n \xrightarrow{n \rightarrow +\infty} 0 \quad \text{and} \quad n\delta_n^4 \xrightarrow{n \rightarrow +\infty} +\infty.$$

381 Additional conditions of this form can obviously be directly integrated in  
382 Theorem 3 to obtain consistency results specific to the corresponding algo-  
383 rithms.

384 Moreover, practitioners generally rely on data based selection of the pa-  
385 rameters of the estimation scheme  $\psi_{\mathcal{D}}$  via a validation method: for instance,  
386 rather than setting  $\delta_n$  to e.g.,  $n^{-5}$  for  $n$  observations (a choice which is com-  
387 patible with theoretical constraints on  $\delta_n$ ), one chooses the value of  $\delta_n$  that



388 optimizes an estimation of the performances of the regression function ob-  
 389 tained on an independent data set (or via a re-sampling approach).

390 In addition to the parameters of the estimation scheme, functional data  
 391 raise the question of the convenient order of the derivative,  $m$ , and of the  
 392 sampling grid optimality. In practical applications, the number of available  
 393 sampling points can be unnecessarily large (see Biau et al. (2005) for an ex-  
 394 ample with more than 8 000 sampling points). The preprocessing performed  
 395 by  $\mathbf{Q}_{\lambda_d, \tau_d}$  do not change the dimensionality of the data which means that  
 396 overfitting can be observed in practice when the number of sampling points  
 397 is large compared to the number of functions. Moreover, processing very  
 398 high dimensional vectors is time consuming. It is there quite interesting in  
 399 practice to use a down-sampled version of the original grid.

400 To select the parameters of  $\psi_D$ , the order of the derivative and/or the  
 401 down-sampled grid, a validation strategy, based on splitting the dataset into  
 402 training and validation sets, could be used. A simple adaptation of the  
 403 idea of Berlinet et al. (2008); Biau et al. (2005); Laloë (2008); Rossi and Villa  
 404 (2006) shows that a penalized validation method can be used to choose any  
 405 combination of those parameters consistently. According to those papers,  
 406 the condition for the consistency of the validation strategy would simply  
 407 relate the shatter coefficients of the set of classifiers in  $\mathbb{R}^d$  to the penalization  
 408 parameter of the validation. Once again, this type of results is a rather direct  
 409 extension of Theorem 3.

## 410 6. Applications

411 In this section, we show that the proposed approach works as expected on  
 412 real world spectrometric examples: for some applications, the use of deriva-  
 413 tives leads to more accurate models than the direct processing of the spectra  
 414 (see e.g. Rossi et al. (2005); Rossi and Villa (2006) for other examples of such  
 415 a behavior based on ad hoc estimators of the spectra derivatives). It should  
 416 be noted that the purpose of this section is only to illustrate the behavior  
 417 of the proposed method on finite datasets. The theoretical results of the  
 418 present paper show that all consistent schemes have asymptotically identical  
 419 performances, and therefore that using derivatives is asymptotically useless.  
 420 On a finite dataset however, preprocessing can have strong influence on the  
 421 predictive performances, as will be illustrated in the present section. In ad-  
 422 dition, schemes that are not universally consistent, e.g., linear models, can  
 423 lead to excellent predictive performances on finite datasets; such models are

therefore included in the present section despite the fact the theory does not apply to them.

### 6.1. Methodology

The methodology followed for the two illustrative datasets is roughly the same:

1. the dataset is randomly split into a training set on which the model is estimated and a test set on which performances are computed. The split is repeated several times. The Tecator dataset (Section 6.2) is rather small (240 spectra) and exhibits a rather large variability in predictive performances between different random splits. We have therefore used 250 random splits. For the Yellow-berry dataset (Section 6.3), we used only 50 splits as the relative variability in performances is far less important.
2.  $\lambda$  is chosen by a global leave-one-out strategy on the spectra contained in training set (as suggested in Section 5.1). More precisely, a leave-one-out estimate of the reconstruction error of the spline approximation of each training spectrum is computed for a finite set of candidate values for  $\lambda$ . Then a common  $\lambda$  is chosen by minimizing the average over the training spectra of the leave-one-out reconstruction errors. This choice is relevant as cross validation estimates of  $\lambda$  are known to have favorable theoretical properties (see Craven and Wahba (1978); Utreras (1981) among others).
3. for regression problems, a Kernel Ridge Regression (KRR) Saunders et al. (1998); Shawe-Taylor and Cristianini (2004) is then performed to estimate the regression function; this method is consistent when used with a Gaussian kernel under additional conditions on the parameters (see Theorem 9.1 of Steinwart and Christmann (2008)); as already explained, in the applications, Kernel Ridge Regression is performed both with a Gaussian kernel and with a linear kernel (in that last case, the model is essentially a ridge regression model). Parameters of the models (a regularization parameter,  $\delta_n$ , in all cases and a kernel parameter,  $\gamma$  for Gaussian kernels) are chosen by a grid search that minimizes a validation based estimate of the performances of the model (on the training set). A leave-one-out solution has been chosen: in Kernel Ridge Regression, the leave-one-out estimate of the performances of

the model is obtained as a by-product of the estimation process, without additional computation cost, see e.g. Cawley and Talbot (2004). Additionally, for a sake of comparison with a more traditional approach in FDA, Kernel Ridge Regression is compared with a nonparametric kernel estimate for the Tecator dataset (Section 6.2.1). Nonparametric kernel estimate is the first nonparametric approach introduced in Functional Data Analysis Ferraty and Vieu (2006) and can thus be seen as a basis for comparison in the context of regression with functional predictors. For this method, the same methodology as with Kernel Ridge Regression was used: the parameter of the model (i.e., the bandwidth) was selected on a grid search minimizing a cross-validation estimate of the performances of the model. In this case, a 4-fold cross validation estimate was used instead of a leave-one-out estimate to avoid a large computational cost.

4. for the classification problem, a Support Vector Machine (SVM) is used Shawe-Taylor and Cristianini (2004). As KRR, SVM are consistent when used with a Gaussian kernel Steinwart (2002). We also use a SVM with a linear kernel as this is quite adapted for classification in high dimensional spaces associated to sampled function data. We also use a K-nearest neighbor model (KNN) for reference. Parameters of the models (a regularization parameter for both SVM, a kernel parameter,  $\gamma$  for Gaussian kernels and number of neighbors  $K$  for KNN) are chosen by a grid search that minimizes a validation based estimate of the classification error: we use a 4-fold cross-validation to get this estimate.
5. We evaluate the models obtained for each random split on the test set. We report the mean and the standard deviation of the performance index (classification error and mean squared error, respectively) and assess the significance of differences between the reported figures via paired Student tests (with level 1%).
6. Finally, we compare models estimated on the raw spectra and on spectra transformed via the  $\mathbf{Q}_{\lambda_d, \tau_d}$  matrix for  $m = 1$  (first derivative) and  $m = 2$  (second derivative). For both values of  $m$ , we used the most classical boundary conditions ( $x(0) = 0$  and  $Dx(0) = 0$ ). Depending of the problem, other boundary conditions could be investigated but this is outside the scope of the present paper (see Besse and Ramsay (1986); Heckman and Ramsay (2000) for discussion on this subject). For the

Tecator problem, we also compare these approaches with models estimated on first and second derivatives based on interpolating splines (i.e. with  $\lambda = 0$ ) and on first and second derivatives estimated by finite differences.

Note that the kind of preprocessing used has almost no impact on the computation time. In general, selecting the parameters of the model with leave-one-out or cross-validation will use significantly more computing power than constructing the splines and calculating their derivatives. For instance, computing the optimal  $\lambda$  with the approach described above takes less than 0.1 second for the Tecator dataset on a standard PC using our R implementation which is negligible compared to the several minutes used to select the optimal parameters of the models used on the preprocessed data.

## 6.2. Tecator dataset

The first studied dataset is the standard Tecator dataset Thodberg (1996)<sup>1</sup>. It consists in spectrometric data from the food industry. Each of the 240 observations is the near infrared absorbance spectrum of a meat sample recorded on a Tecator Infratec Food and Feed Analyzer. Each spectrum is sampled at 100 wavelengths uniformly spaced in the range 850–1050 nm. The composition of each meat sample is determined by analytic chemistry and percentages of moisture, fat and protein are associated this way to each spectrum.

The Tecator dataset is a widely used benchmark in Functional Data Analysis, hence the motivation for its use for illustrative purposes. More precisely, in Section 6.2.1, we address the original regression problem by predicting the percentage of fat content from the spectra with various regression method and various estimates of the derivative preprocessing: this analysis shows that both the method and the use of derivative have a strong effect on the performances whereas the way the derivatives are estimated has almost no effect. Additionally, in Section 6.2.2, we apply a noise (with various variances) to the original spectra in order to study the influence of smoothing in the case of noisy predictors: this section shows the relevance of the use of a smoothing spline approach when the data are noisy. Finally, Section 6.2.3 deals with a classification problem derived from the original Tecator problem

---

<sup>1</sup>Data are available on statlib at <http://lib.stat.cmu.edu/datasets/tecator>

(in the same way as what was done in Ferraty and Vieu (2003)): conclusions of this section are similar to the ones of the regression study.

### 6.2.1. Fat content prediction

As explained above, we first address the regression problem that consists in predicting the fat content of peaces of meat from the Tecator dataset. The parameters of the model are optimized with a grid search using the leave-one-out estimate of the predictive performances (both models use a regularization parameter, with an additional width parameter in the Gaussian kernel case). The original data set is split randomly into 160 spectra for learning and 80 spectra for testing. As shown in the result Table 1, the data exhibit a rather large variability; we use therefore 250 random split to assess the differences between the different approaches.

The performance indexes are the mean squared error (M.S.E.) and the  $R^2$ .<sup>2</sup> As a reference, the target variable (fat) has a variance equal to 14.36. Results are summarized in Table 1.

The first conclusion is that the method itself has a strong effect on the performances of the prediction: for this application, a linear method is not appropriate (mean squared errors are much greater for linear methods than for the kernel ridge regression used with a Gaussian kernel) and the non-parametric kernel estimate gives worse performances than the kernel ridge regression (indeed, they are about 10 times worse). Nevertheless, for non-parametric approaches (Gaussian KKR and NKE), the use of derivatives has also a strong impact on the performances: for kernel ridge regression, e.g., preprocessing by estimating the first order derivative leads to a strong decrease of the mean squared error.

Differences between the average MSEs are not always significant, but we can nevertheless rank the methods in increasing order of modeling error (using notations explained in Table 1) for Gaussian kernel ridge regression:

$$\text{FD1} \leq \text{IS1} \leq \text{S1} < \text{DF2} \leq \text{SS2} < \text{IS2} < \text{O}$$

where  $<$  corresponds to a significant difference (for a paired Student test with level 1%) and  $\leq$  to a non significant one. In this case, the data are very smooth and thus the use of smoothing splines instead of a finite differences

---

<sup>2</sup> $R^2 = 1 - \frac{\text{M.S.E}}{\text{Var}(y)}$  where  $\text{Var}(y)$  is the (empirical) variance of the target variable on the test set.

Method	Data	Average M.S.E. and SD	Average $R^2$
KRR Linear	O	8.69 (4.47)	95.7%
	S1	8.09 (3.85)	96.1%
	IS1	8.09 (3.85)	96.1%
	FD1	8.27 (4.17)	96.0%
	S2	9.64 (4.98)	95.3%
	IS2	9.87 (5.84)	95.2%
	FD2	8.45 (4.18)	95.9%
KRR Gaussian	O	5.02 (11.47)	97.6%
	S1	0.485 (0.385)	99.8%
	IS1	0.485 (0.385)	99.8%
	FD1	<b>0.484</b> (0.387)	<b>99.8%</b>
	S2	0.584 (0.303)	99.7%
	IS2	0.586 (0.303)	99.7%
	FD2	0.569 (0.281)	99.7%
NKE	O	73.1 (16.5)	64.2%
	S1	4.59 (1.09)	97.7%
	IS1	4.59 (1.09)	97.7%
	FD1	4.59 (1.09)	97.7%
	S2	3.75 (1.22)	98.2%
	IS2	3.75 (1.22)	98.2%
	FD2	3.67 (1.18)	98.2%

Table 1: Summary of the performances of the chosen models on the test set (fat Tecator regression problem) when using either a kernel ridge regression (KRR) with linear kernel or with Gaussian kernel or when using a nonparametric kernel estimate (NKE) with various inputs: O (original data), S1 (smoothing splines with order 1 derivatives), IS1 (interpolating splines with order 1 derivatives), FD1 (order 1 derivatives estimated by finite differences) and S2, IS2 and FD2 (the same as previously with order 2 derivatives).

approximation does not have a significant impact on the predictions. However, in this case, the roughest approach, consisting in the estimation of the derivatives by finite differences, gives the best performances.

### 6.2.2. Noisy spectra

This section studies the situation in which functional data observations are corrupted by noise. This is done by adding a noise to each spectrum of the Tecator dataset. More precisely, each spectrum has been corrupted by

$$X_i^b(t) = X_i(t) + \epsilon_{it} \quad (9)$$

where  $(\epsilon_{it})$  are i.i.d. Gaussian variables with standard deviation equal to either 0.01 (small noise) or to 0.2 (large noise). 10 observations of the data generated this way are given in Figure 2.

The same methodology as for the non noisy data has been applied to  $(X_i^b)$  to predict the fat content. The experiments have been restricted to the use of kernel ridge regression with a Gaussian kernel (according to the nonlinearity of the problem shown in the previous section). Results are summarized in Table 2 and Figure 3.

In addition, the results can be ranked this way:

#### Noise with sd equal to 0.01

$$S2 < S1 < IS1 \leq O < FD1 < IS2 \leq FD2$$

#### Noise with sd equal to 0.2

$$S1 < O < S2 < FD1 < IS1 < IS2 \leq FD2$$

where  $<$  corresponds to a significant difference (for a paired Student test with level 1%).

The first conclusion of these experiments is that, even though the derivatives are the relevant predictors, their performances are strongly affected by the noise (compared to the ones of the original data: note that the average M.S.E. reported in Table 1 are more 10 times lower than the best ones from Table 2 and that, in the best cases,  $R^2$  is slightly greater than 50% for the most noisy dataset). In particular, using interpolating splines or finite difference derivatives leads to highly deteriorated performances. In this situation, the approach proposed in the paper is particularly useful and helps to keep

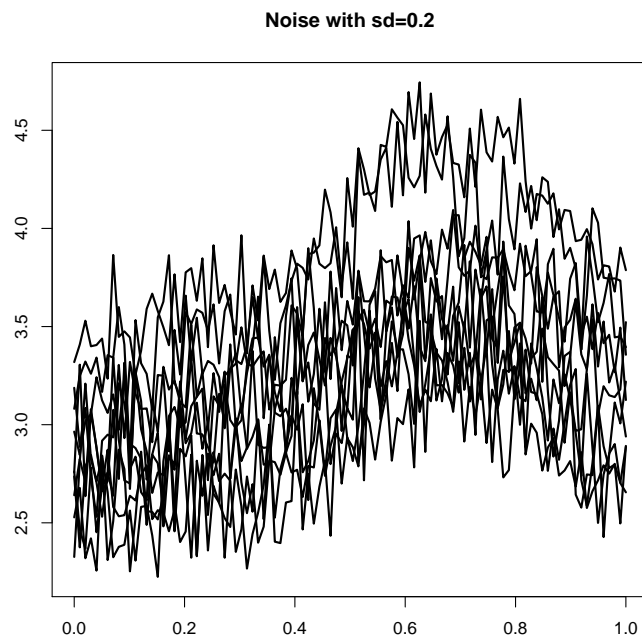
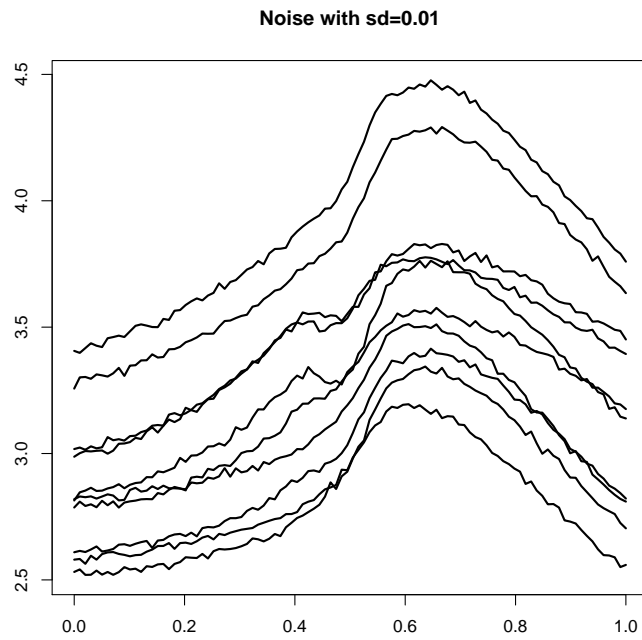


Figure 2: 10 observations of the noisy data generated from the Tecator spectra as in Equation 9



Noise	Data	Average M.S.E. and SD	Average $R^2$
sd = 0.01	O	13.3 (13.5)	93.5%
	S1	7.45 (1.5)	96.4%
	IS1	12.72 (2.2)	93.8%
	FD1	20.03 (2.8)	90.3%
	S2	<b>6.83</b> (1.4)	<b>96.7%</b>
	IS2	31.23 (5.9)	84.9%
	FD2	31.10 (5.9)	84.9%
sd = 0.2	O	87.9 (13.9)	57.4%
	S1	<b>85.0</b> (12.5)	<b>58.8%</b>
	IS1	210.1 (36.1)	-1.9%
	FD1	209.1 (33.0)	-1.4%
	S2	95.9 (12.8)	53.5%
	IS2	213.7 (33.1)	-3.6%
	FD2	235.1 (222.7)	-14.0%

Table 2: Summary of the performances of the chosen models on the test set (fat Tecator regression problem) with noisy spectra.

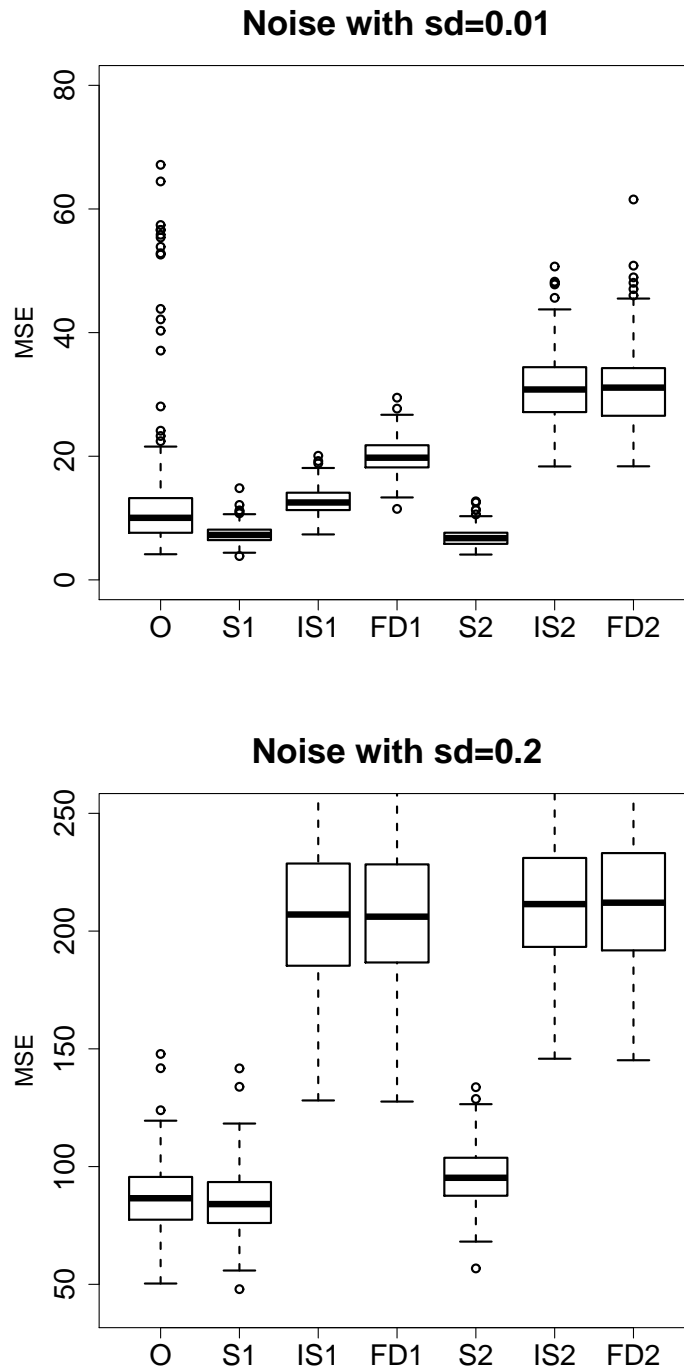


Figure 3: Mean squared errors boxplot for the noisy fat Tecator regression problem with Gaussian kernel (the worst test samples for IS and FD have been removed for a sake of clarity)

586 better performances than with the original data. Indeed, the differences of  
587 the smoothing splines approach with the original data is still significant (for  
588 both derivatives in the “small noise” case and for the first order derivative  
589 in the “high noise” case), even though, the most noisy the data are, the  
590 most difficult it is to estimate the derivatives in an accurate way. That is,  
591 except for smoothing spline derivatives, the estimation of the derivatives for  
592 the most noisy dataset is so bad that it leads to negative  $R^2$  when used in  
593 the regression task.

### 594 6.2.3. *Fat content classification*

595 In this section, the fat content regression problem is transformed into a  
596 classification problem. To avoid imbalance in class sizes, the median value  
597 of the fat in the dataset is used as the splitting criterion: the first class  
598 consists in 119 samples with strictly less than 13.5 % of fat, while the second  
599 class contains the other 121 samples with a fat content equal or higher than  
600 13.5 %.

601 As in previous sections, the analysis is conducted on 250 random splits of  
602 the dataset into 160 learning spectra and 80 test spectra. We used stratified  
603 sampling: the test set contains 40 examples from each class. The 4 fold  
604 cross-validation used to select the parameters of the models on the learning  
605 set is also stratified with roughly 20 examples of each class in each fold.

606 The performance index is the mis-classification rate (MCR) on the test  
607 set, reported in percentage and averaged over the 250 random splits. Results  
608 are summarized in Table 3. As in the previous sections, both the model  
609 and the preprocessing have some influence on the results. In particular,  
610 using derivatives always improves the classification accuracy while the actual  
611 method used to compute those derivatives has no particular influence on the  
612 results. Additionally, using interpolation splines leads, in this particular  
613 problem, to results that are exactly identical to the ones obtained with the  
614 smoothing splines: they are not reported in Table 3.

615 More precisely, for the three models (linear SVM, Gaussian SVM and  
616 KNN), differences in mis-classification rates between the smoothing spline  
617 preprocessing and the finite differences calculation is never significant, ac-  
618 cording to a Student test with level 1 %. Additionally while the actual aver-  
619 age mis-classification rates might seem quite different, the large variability of  
620 the results (shown by the standard deviations) leads to significant differences  
621 only for the most obvious cases. In particular, SVM models using derivatives  
622 (of order one or two) are indistinguishable one from another using a Student

Method	Data	Average MCR	SD of MCR
Linear SVM	O	1.41	1.55
	S1	<b>0.73</b>	1.15
	FD1	0.74	1.15
	S2	0.94	1.27
	FD2	0.92	1.23
Gaussian SVM	O	3.39	2.57
	S1	0.97	1.41
	FD1	0.98	1.42
	S2	0.99	2.00
	FD2	0.97	1.27
KNN	O	22.0	5.02
	S1	6.67	2.55
	FD1	6.57	2.55
	S2	1.93	1.65
	FD2	1.93	1.63

Table 3: Summary of the performances of the chosen models on the test set (Tecator fat classification problem). See Table 1 for notations. MCR stands for mis-classification rate, SD for standard deviation.

623 test with level 1 %: all methods with less than 1 % of mean mis-classification  
 624 rate perform essentially identically. Other differences are significant: for in-  
 625 stance the linear SVM used on raw data performs significantly worse than  
 626 any SVM model used on derivatives.

627 It should be noted that the classification task studied in the present sec-  
 628 tion is obviously simpler than the regression task from which it is derived.  
 629 This explains the very good predictive performances obtained by simple mod-  
 630 els such as a linear SVM, especially with the proper preprocessing.

### 631 6.3. Yellow-berry dataset

632 The goal of the last experiment is to predict the presence of yellow-berry in  
 633 durum wheat (*Triticum durum*) kernels via a near infrared spectral analysis  
 634 (see Figure 4). Yellow-berry is a defect of the durum wheat seeds that reduces  
 635 the quality of the flour produced from affected wheat. The traditional way  
 636 to assess the occurrence of yellow-berry is by visual analysis of a sample of  
 637 the seed stock. In the current application, a quality measure related to the  
 638 occurrence of yellow-berry is predicted from the spectrum of the seed.

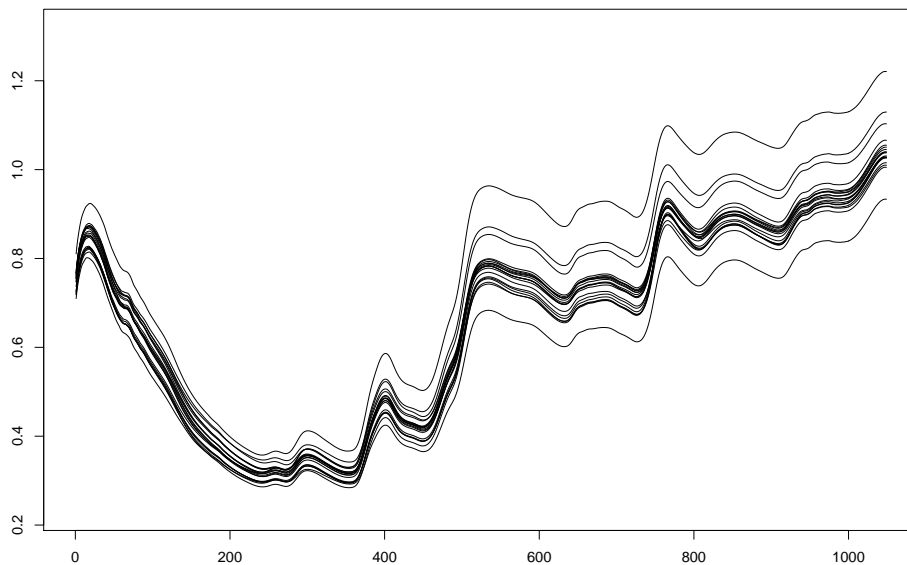


Figure 4: 20 observations of NIR spectra of durum wheat

639 The dataset consists in 953 spectra sampled at 1049 wavelengths uni-  
640 formly spaced in the range 400–2498 nm. The dataset is split randomly into  
641 600 learning spectra and 353 test spectra. Comparatively to the Tecator  
642 dataset, the variability of the results is smaller in the present case. We used  
643 therefore 50 random splits rather than 250 in the previous section.

644 The regression models were build via a Kernel Ridge Regression approach  
645 using a linear kernel and a Gaussian kernel. In both cases, the regularization  
646 parameter of the model is optimized by a leave-one-out approach. In addi-  
647 tion, the width parameter of the Gaussian kernel is optimized via the same  
648 procedure at the same time.

649 The performance index is the mean squared error (M.S.E.). As a refer-  
650 ence, the target variable has a variance of 0.508. Results are summarized in  
Table 4 and Figure 5.

Kernel and Data	Average M.S.E.	Standard deviation	Average $R^2$
Linear-O	0.122	$8.77 \cdot 10^{-3}$	76.1%
Linear-S1	0.138	$9.53 \cdot 10^{-3}$	73.0%
Linear-S2	0.122	$8.41 \cdot 10^{-3}$	76.1%
Gaussian-O	0.110	$20.2 \cdot 10^{-3}$	78.5%
Gaussian-S1	0.0978	$7.92 \cdot 10^{-3}$	80.9%
Gaussian-S2	0.0944	$8.35 \cdot 10^{-3}$	81.5%

Table 4: Summary of the performances of the chosen models on the test set (durum wheat regression problem)

651  
652 As in the previous section, we can rank the methods in increasing order  
653 of modelling error, we obtain the following result:

$$\text{G-S2} < \text{G-S1} < \text{G-O} < \text{L-O} \leq \text{L-S2} < \text{L-S1},$$

654 where G stands for Gaussian kernel and L for linear kernel (hence G-S2 stands  
655 for kernel ridge regression with gaussian kernel and smoothing splines with  
656 order 2 derivatives);  $<$  corresponds to a significant difference (for a paired  
657 Student test with level 1%) and  $\leq$  to a non significant one. For this appli-  
658 cation, there is a significant gain in using a non linear model (the Gaussian  
659 kernel). In addition, the use of derivatives leads to less contrasted perfor-  
660 mances that the ones obtained in the previous section but it still improves  
661 the quality of the non linear model in a significant way. In term of normal-  
662 ized mean squared error (mean squared error divided by the variance of the

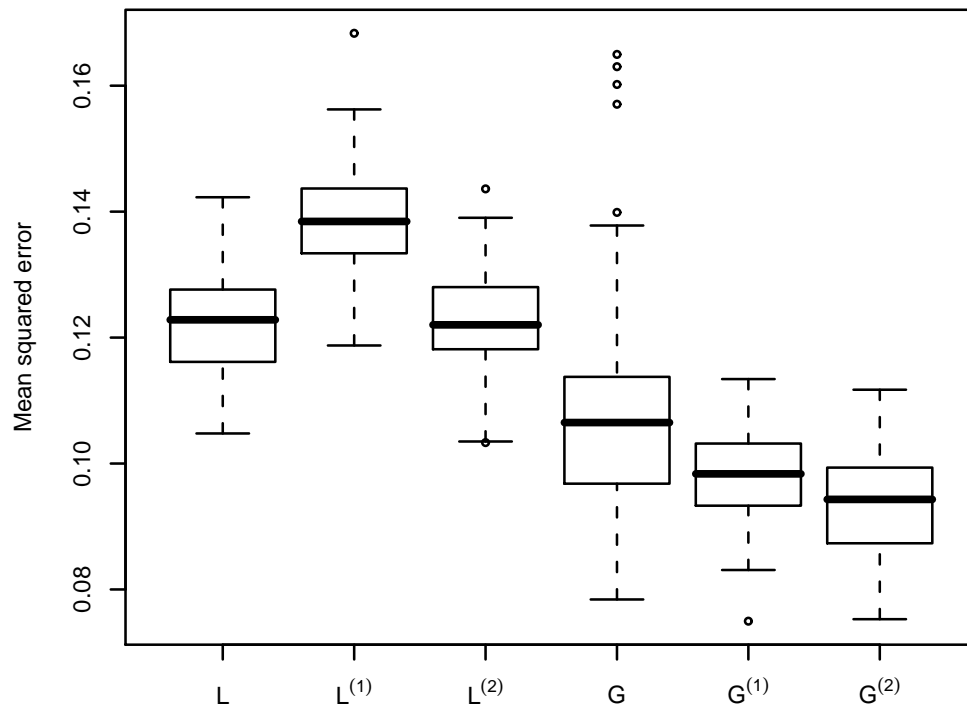


Figure 5: Mean squared error boxplots for the “durum wheat” regression problem (see Table 4 for the full names of the regression models)

target variable), using a non linear model with the second derivatives of the spectra corresponds to an average gain of more than 5% (i.e., a reduction of the normalised mean squared error from 24% for the standard linear model to 18.6%).

## 7. Conclusion

In this paper we proposed a theoretical analysis of a common practice that consists in using derivatives in classification or regression problems when the predictors are curves. Our method relies on smoothing splines reconstruction of the functions which are known only via a discrete deterministic sampling. The method is proved to be consistent for very general classifiers or regression schemes: it reaches asymptotically the best risk that could have been obtained by constructing a regression/classification model on the true random functions.

We have validated the approach by combining it with nonparametric regression and classification algorithms to study two real-world spectrometric datasets. The results obtained in these applications confirm once again that relying on derivatives can improve the quality of predictive models compared to a direct use of the sampled functions. The way the derivatives are estimated does not have a strong impact on the performances except when the data are noisy. In this case, the use of smoothing splines is quite relevant.

In the future, several issues could be addressed. An important practical problem is the choice of the best order of the derivative,  $m$ . We consider that a model selection approach relying on a penalized error loss could be used, as is done, in e.g., Rossi and Villa (2006), to select the dimension of truncated basis representation for functional data. Note that in practice, such parameter selection method could lead to select  $m = 0$  and therefore to automatically exclude derivative calculation when it is not needed. This will extend the application range of the proposed model.

A second important point to study is the convergence rate for the method. It would be very convenient for instance, to be able to relate the size of the sampling grid to the number of functions. But, this latter issue would require the use of additional assumptions on the smoothness of the regression function whereas the result presented in this paper, even if more limited, only needs mild conditions.



## 697 8. Acknowledgement

698 We thank Cécile Levasseur and Sylvain Coulomb (École d'Ingénieurs de  
699 Purpan, EIP, Toulouse, France) for sharing the interesting problem presented  
700 in Section 6.3.

701 We also thank Philippe Besse (Institut de Mathématiques de Toulouse,  
702 Université de Toulouse, France) for helpfull discussions and suggestions.

703 Finally, we thank the anonymous reviewers for their valuable comments  
704 and suggestions that helped to improve the quality of the paper.

## 705 References

706 Bahlmann, C., Burkhardt, H., 2004. The writer independent online hand-  
707 writing recognition system *frog on hand* and cluster generative statistical  
708 dynamic time warping. IEEE Transactions on Pattern Analysis and Ma-  
709 chine Intelligence 26, 299–310.

710 Berline, A., Biau, G., Rouvière, L., 2008. Functional supervised classifica-  
711 tion with wavelets. Annales de l'ISUP 52, 61–80.

712 Berline, A., Thomas-Agnan, C., 2004. Reproducing Kernel Hilbert Spaces  
713 in Probability and Statistics. Kluwer Academic Publisher.

714 Besse, P., Ramsay, J., 1986. Principal component analysis of sampled curves.  
715 Psychometrika 51, 285–311.

716 Biau, G., Bunea, F., Wegkamp, M., 2005. Functional classification in Hilbert  
717 spaces. IEEE Transactions on Information Theory 51, 2163–2172.

718 Cardot, H., Ferraty, F., Sarda, P., 1999. Functional linear model. Statistics  
719 and Probability Letters 45, 11–22.

720 Cawley, G., Talbot, N., 2004. Fast exact leave-one-out cross-validation of  
721 sparse least-squares support vector machines. Neural Networks 17, 1467–  
722 1475.

723 Cox, D., 1984. Multivariate smoothing splines functions. SIAM Journal on  
724 Numerical Analysis 21, 789–813.

725 Craven, P., Wahba, G., 1978. Smoothing noisy data with spline functions.  
726 Numerische Mathematik 31, 377–403.

- 727 Dauxois, J., Pousse, A., 1976. Les analyses factorielles en calcul des proba-  
 728 bilités et en statistique : essai d'étude synthétique. Thèse d'État. Univer-  
 729 sité Toulouse III.
- 730 Dejean, S., Martin, P., Baccini, A., Besse, P., 2007. Clustering time-series  
 731 gene expression data using smoothing spline derivatives. EURASIP Jour-  
 732 nal on Bioinformatics and Systems Biology 2007, Article ID70561.
- 733 Deville, J., 1974. Méthodes statistiques et numériques de l'analyse har-  
 734 monique. Annales de l'INSEE 15, 3–97.
- 735 Devroye, L., Györfi, L., 1985. Nonparametric Density Estimation: the  $L_1$   
 736 view. John Wiley, New York.
- 737 Devroye, L., Györfi, L., Krzyżak, A., Lugosi, G., 1994. On the strong uni-  
 738 versal consistancy of nearest neighbor regression function estimates. The  
 739 Annals of Statistics 22, 1371–1385.
- 740 Devroye, L., Györfi, L., Lugosi, G., 1996. A Probabilistic Theory for Pattern  
 741 Recognition. Springer-Verlag, New York.
- 742 Devroye, L., Krzyżak, A., 1989. An equivalence theorem for  $l_1$  convergence  
 743 of the kernel regression estimate. Journal of Statistical Planning and In-  
 744 ference 23, 71–82.
- 745 Faragó, T., Györfi, L., 1975. On the continuity of the error distortion func-  
 746 tion for multiple-hypothesis decisions. IEEE Transactions on Information  
 747 Theory 21, 458–460.
- 748 Ferraty, F., Vieu, P., 2003. Curves discrimination: a non parametric ap-  
 749 proach. Computational and Statistical Data Analysis 44, 161–173.
- 750 Ferraty, F., Vieu, P., 2006. NonParametric Functional Data Analysis.  
 751 Springer.
- 752 Ferré, L., Yao, A., 2003. Functional sliced inverse regression analysis. Statis-  
 753 tics 37, 475–488.
- 754 Györfi, L., Kohler, M., Krzyżak, A., Walk, H., 2002. A Distribution-Free  
 755 Theory of Nonparametric Regression. Springer, New York.

- 756 Heckman, N., Ramsay, J., 2000. Penalized regression with model-based  
757 penalties. *The Canadian Journal of Statistics* 28, 241–258.
- 758 James, G., 2002. Generalized linear models with functional predictor vari-  
759 ables. *Journal of the Royal Statistical Society Series B* 64, 411–432.
- 760 James, G., Hastie, T., 2001. Functional linear discriminant analysis for ir-  
761 regularly sampled curves. *Journal of the Royal Statistical Society, Series*  
762 *B* 63, 533–550.
- 763 James, G., Hastie, T., Sugar, C., 2000. Principal component models for  
764 sparse functional data. *Biometrika* 87, 587–602.
- 765 James, G., Silverman, B., 2005. Functional adaptive model estimation. *Jour-*  
766 *nal of the American Statistical Association* 100, 565–576.
- 767 Kallenberg, O., 1997. *Foundations of Modern Probability. Probability and*  
768 *its Applications*, Springer.
- 769 Kimeldorf, G., Wahba, G., 1971. Some results on Tchebycheffian spline  
770 functions. *Journal of Mathematical Analysis and Applications* 33, 82–95.
- 771 Laloë, T., 2008. A k-nearest neighbor approach for functional regression.  
772 *Statistics and Probability Letters* 78, 1189–1193.
- 773 Lugosi, G., Zeger, K., 1990. Nonparametric estimation via empirical risk  
774 minimization. *IEEE Transaction on Information Theory* 41, 677–687.
- 775 Mas, A., Pumo, B., 2009. Functional linear regression with derivatives. *Jour-*  
776 *nal of Nonparametric Statistics* 21, 19–40. Submitted: under revision.  
777 Available at <http://www.math.univ-montp2.fr/~mas/FLRD.pdf>.
- 778 Pollard, D., 2002. *A User’s Guide to Measure Theoretic Probability*. Cam-  
779 *bridge University Press*, Cambridge.
- 780 Ragozin, D., 1983. Error bounds for derivative estimation based on spline  
781 smoothing of exact or noisy data. *Journal of Approximation Theory* 37,  
782 335–355.
- 783 Ramsay, J., Dalzell, C., 1991. Some tools for functional data analysis (with  
784 discussion). *Journal of the Royal Statistical Society. Series B. Statistical*  
785 *Methodology* 53, 539–572.

- 786 Ramsay, J., Silverman, B., 1997. Functional Data Analysis. Springer Verlag,  
787 New York.
- 788 Ramsay, J., Silverman, B., 2002. Applied Functional Data Analysis. Springer  
789 Verlag.
- 790 Rossi, F., Conan-Guez, B., 2005. Functional multi-layer perceptron: a non-  
791 linear tool for functional data anlysis. Neural Networks 18, 45–60.
- 792 Rossi, F., Conan-Guez, B., 2006. Theoretical properties of projection based  
793 multilayer perceptrons with functional inputs. Neural Processing Letters  
794 23, 55–70.
- 795 Rossi, F., Delannay, N., Conan-Guez, B., Verleysen, M., 2005. Representa-  
796 tion of functional data in neural networks. Neurocomputing 64, 183–210.
- 797 Rossi, F., Villa, N., 2006. Support vector machine for functional data classi-  
798 fication. Neurocomputing 69, 730–742.
- 799 Saunders, G., Gammerman, A., Vovk, V., 1998. Ridge regression learning  
800 algorithm in dual variables, in: Proceedings of the Fifteenth International  
801 Conference on Machine Learning (ICML’98), Madison, Wisconsin, USA.  
802 pp. 515–521.
- 803 Shawe-Taylor, J., Cristianini, N., 2004. Kernel methods for pattern analysis.  
804 Cambridge University Press, Cambridge, UK.
- 805 Steinwart, I., 2002. Support vector machines are universally consistent. Jour-  
806 nal of Complexity 18, 768–791.
- 807 Steinwart, I., Christmann, A., 2008. Support Vector Machines. Information  
808 Science and Statistics, Springer.
- 809 Thodberg, H., 1996. A review of bayesian neural network with an application  
810 to near infrared spectroscopy. IEEE Transaction on Neural Networks 7,  
811 56–72.
- 812 Utreras, F., 1981. Optimal smoothing of noisy data using spline functions.  
813 SIAM Journal on Scientific Computing 2, 153–163.
- 814 Utreras, F., 1988. Boundary effects on convergence rates for Tikhonov regu-  
815 larization. Journal of Approximation Theory 54, 235–249.

- 816 Wahba, G., 1990. Spline Models for Observational Data. Society for Indus-  
817 trial and Applied Mathematics, Philadelphia, Pennsylvania.
- 818 Williams, B., Toussaint, M., Storkey, A., 2006. Extracting motion primitives  
819 from natural handwriting data, in: In Proceedings of the International  
820 Conference on Artificial Neural Networks (ICANN).
- 821 Zhao, L., 1987. Exponential bounds of mean error for the nearest neighbor  
822 estimates of regression functions. Journal of Multivariate Analysis 21,  
823 168–178.

## 824 9. Proofs

### 825 9.1. Theorem 1

826 In the original theorem (Lemma 3.1) in Kimeldorf and Wahba (1971),  
827 one has to verify that  $(k_0(t_l, \cdot))_l$  spans  $\mathcal{H}_0^m$  and that  $(k_1(t_l, \cdot))_l$  are linearly  
828 independent. These are consequences of Assumption (A1).

829 First,  $k_0(s, t) = \sum_{i,j=0}^{m-1} b_{ij}^{(-1)} s^i t^j$  where  $\tilde{B} = (b_{i,j}^{(-1)})_{i,j}$  is the in-  
830 verse of  $(\sum_{l=1}^m B^l s^i B^l t^j)_{i,j}$  (see Heckman and Ramsay (2000)). Then  
831  $(k_0(t_1, s), \dots, k_0(t_{|\tau_d|}, s)) = (1, s, \dots, s^{m-1}) \tilde{B} [V_{m-1}(t_1, \dots, t_{|\tau_d|})]^T$  where  
832  $V_{m-1}(t_1, \dots, t_{|\tau_d|})$  is the Vandermonde matrix with  $m - 1$  columns and  $|\tau_d|$   
833 rows associated to values  $t_1, \dots, t_{|\tau_d|}$ . If the  $(t_l)_l$  are distinct, this matrix is  
834 of full rank.

835 Moreover the reproducing property shows that  $\sum_{l=1}^{|\tau_d|} a_l k_1(t_l, \cdot) \equiv 0$  im-  
836 plies  $\sum_{l=1}^{|\tau_d|} a_l f(t_l) \equiv 0$  for all  $f \in \mathcal{H}_1^m$ . Hence,  $\mathcal{H}_1^m = \text{Ker}(B^T, \sum_{l=1}^{|\tau_d|} a_l \zeta_l)^T$   
837 where  $\zeta_l$  denotes the linear form  $h \in \mathcal{H}^m \rightarrow h(t_l)$ . As the co-dimension of  
838  $\mathcal{H}_1^m$  is  $\dim \mathcal{H}_0^m = m$  and as, by Assumption (A1),  $B$  is linearly independent  
839 of  $\sum_{l=1}^{|\tau_d|} a_l \zeta_l$ , we thus have  $\sum_{l=1}^{|\tau_d|} a_l \zeta_l \equiv 0$  (or  $\text{codim Ker}(B^T, \sum_{l=1}^{|\tau_d|} a_l \zeta_l)^T =$   
840  $\dim \text{Im}(B^T, \sum_{l=1}^{|\tau_d|} a_l \zeta_l)$  would be  $m+1$ ). Thus, we obtain that  $\sum_{l=1}^{|\tau_d|} a_l f(t_l) \equiv$   
841  $0$  for all  $f$  in  $\mathcal{H}^m$  and, as  $(t_l)$  are distinct, that  $a_l = 0$  for all  $l$ , leading to the  
842 independence conclusion for the  $(k_1(t_l, \cdot))_l$ .

843 Finally, we prove that  $\mathcal{S}_{\lambda, \tau_d}$  is of full rank. Indeed, if  $\mathcal{S}_{\lambda, \tau_d} \mathbf{x}^{\tau_d} = 0$ ,  
844  $\omega^T M_0 \mathbf{x}^{\tau_d} = 0$  and  $\eta^T M_1 \mathbf{x}^{\tau_d} = 0$ . As  $(\omega_k)_k$  is a basis of  $\mathcal{H}_0^m$ ,  $\omega^T M_0 \mathbf{x}^{\tau_d} = 0$   
845 implies  $M_0 \mathbf{x}^{\tau_d} = 0$  and therefore  $M_1 = (K_1 + \lambda I_d)^{-1}$ . As shown above,  
846 the  $(k_1(t_l, \cdot))_l$  are linearly independent and therefore  $\eta M_1 \mathbf{x}^{\tau_d} = 0$  implies  
847  $M_1 \mathbf{x}^{\tau_d} = 0$ , which in turns leads to  $\mathbf{x}^{\tau_d} = 0$  via the simplified formula for  $M_1$ .

848 *9.2. Corollary 1*

849 We give only the proof for the classification case, the regression case is  
850 identical.

851 According to Theorem 1, there is a full rank linear mapping from  $\mathbb{R}^{|\tau_d|}$   
852 to  $\mathcal{H}^m$ ,  $\mathcal{S}_{\lambda, \tau_d}$ , such that for any function  $x \in \mathcal{H}^m$ ,  $\hat{x}_{\lambda, \tau_d} = \mathcal{S}_{\lambda, \tau_d} \mathbf{x}^{\tau_d}$ . Let  
853 us denote  $\mathcal{I}_{\lambda, \tau_d}$  the image of  $\mathbb{R}^{|\tau_d|}$  by  $\mathcal{S}_{\lambda, \tau_d}$ ,  $\mathbf{P}_{\lambda, \tau_d}$  the orthogonal projection  
854 from  $\mathcal{H}^m$  to  $\mathcal{I}_{\lambda, \tau_d}$  and  $\mathcal{S}_{\lambda, \tau_d}^{-1}$  the inverse of  $\mathcal{S}_{\lambda, \tau_d}$  on  $\mathcal{I}_{\lambda, \tau_d}$ . Obviously, we have  
855  $\mathcal{S}_{\lambda, \tau_d}^{-1} \circ \mathbf{P}_{\lambda, \tau_d}(\hat{x}_{\lambda, \tau_d}) = \mathbf{x}^{\tau_d}$ .

856 Let  $\psi$  be a measurable function from  $\mathbb{R}^{|\tau_d|}$  to  $\{-1, 1\}$ . Then  $\zeta_\psi$  de-  
857 fined on  $\mathcal{H}^m$  by  $\zeta_\psi(u) = \psi(\mathcal{S}_{\lambda, \tau_d}^{-1} \circ \mathbf{P}_{\lambda, \tau_d}(u))$  is a measurable function from  
858  $\mathcal{H}^m$  to  $\{-1, 1\}$  (because  $\mathcal{S}_{\lambda, \tau_d}^{-1}$  and  $\mathbf{P}_{\lambda, \tau_d}$  are both continuous). Then for  
859 any measurable  $\psi$ ,  $\inf_{\phi: \mathcal{H}^m \rightarrow \{-1, 1\}} \mathbb{P}(\phi(\hat{X}_{\lambda, \tau_d}) \neq Y) \leq \mathbb{P}(\zeta_\psi(\hat{X}_{\lambda, \tau_d}) \neq Y) =$   
860  $\mathbb{P}(\psi(\mathbf{X}^{\tau_d}) \neq Y)$ , and therefore

$$\inf_{\phi: \mathcal{H}^m \rightarrow \{-1, 1\}} \mathbb{P}(\phi(\hat{X}_{\lambda, \tau_d}) \neq Y) \leq \inf_{\phi: \mathbb{R}^{|\tau_d|} \rightarrow \{-1, 1\}} \mathbb{P}(\phi(\mathbf{X}^{\tau_d}) \neq Y). \quad (10)$$

861 Conversely, let  $\psi$  be a measurable function from  $\mathcal{H}^m$  to  $\{-1, 1\}$ . Then  $\zeta_\psi$  de-  
862 fined on  $\mathbb{R}^{|\tau_d|}$  by  $\zeta_\psi(\mathbf{u}) = \psi(\mathcal{S}_{\lambda, \tau_d}(\mathbf{u}))$ , is measurable. Then for any measurable  
863  $\psi$ ,  $\inf_{\phi: \mathbb{R}^{|\tau_d|} \rightarrow \{-1, 1\}} \mathbb{P}(\phi(\mathbf{X}^{\tau_d}) \neq Y) \leq \mathbb{P}(\zeta_\psi(\mathbf{X}^{\tau_d}) \neq Y) = \mathbb{P}(\psi(\hat{X}_{\lambda, \tau_d}) \neq Y)$ ,  
864 and therefore

$$\inf_{\phi: \mathbb{R}^{|\tau_d|} \rightarrow \{-1, 1\}} \mathbb{P}(\phi(\mathbf{X}^{\tau_d}) \neq Y) \leq \inf_{\phi: \mathcal{H}^m \rightarrow \{-1, 1\}} \mathbb{P}(\phi(\hat{X}_{\lambda, \tau_d}) \neq Y). \quad (11)$$

865 The combination of equations (10) and (11) gives equality (4).

866 *9.3. Corollary 3*

867 **1. Suppose assumption (A4a) is fulfilled**

868 The proof is based on Theorem 1 in Faragó and Györfi (1975). This  
869 theorem relates the Bayes risk of a classification problem based on  
870  $(X, Y)$  with the Bayes risk of the problem  $(T_d(X), Y)$  where  $(T_d)$  is a  
871 series of transformations on  $X$ .

872 More formally, for a pair of random variables  $(X, Y)$ , where  $X$  takes  
873 values in  $\mathcal{X}$ , an arbitrary metric space, and  $Y$  in  $\{-1, 1\}$ , let us

874 denote for any series of functions  $T_d$  from  $\mathcal{X}$  to itself,  $L^*(T_d) =$   
875  $\inf_{\phi: \mathcal{X} \rightarrow \{-1,1\}} \mathbb{P}(\phi(T_d(X)) \neq Y)$ . Theorem 1 from Faragó and Györfi  
876 (1975) states that  $\mathbb{E}(\delta(T_d(X), X)) \xrightarrow{d \rightarrow +\infty} 0$  implies  $L^*(T_d) \xrightarrow{d \rightarrow +\infty} L^*$ ,  
877 where  $\delta$  denotes the metric on  $\mathcal{X}$ .

878 This can be applied to  $\mathcal{X} = (\mathcal{H}^m, \langle \cdot, \cdot \rangle_{L^2})$  with  $T_d(X) =$   
879  $\hat{X}_{\lambda_d, \tau_d} = S_{\lambda_d, \tau_d} \mathbf{X}^{\tau_d}$ : under Assumptions (A1) and (A2), Theo-  
880 rem 2 gives:  $\|T_d(X) - X\|_{L^2}^2 \leq \left( A_{R,m} \lambda_d + B_{R,m} \frac{1}{|\tau_d|^{2m}} \right) \|D^m X\|_{L^2}^2$ .  
881 Taking the expectation of both sides gives  $\mathbb{E}(\|T_d(X) - X\|_{L^2}^2) \leq$   
882  $\left( A_{R,m} \lambda_d + B_{R,m} \frac{1}{|\tau_d|^{2m}} \right) \mathbb{E}(\|D^m X\|_{L^2}^2)$ , using the fact that the constants  
883 are independent of the function under analysis. Then under Assump-  
884 tions (A4a) and (A3),  $\mathbb{E}(\|T_d(X) - X\|_{L^2}^2) \xrightarrow{d \rightarrow +\infty} 0$ . According to  
885 Faragó and Györfi (1975), this implies  $\lim_{d \rightarrow \infty} L_d^* = L^*$ .

## 886 2. Suppose assumption (A4b) is fulfilled

887 The conclusion will follow both for classification case and for regres-  
888 sion case. The proof follows the general ideas of Biau et al. (2005);  
889 Rossi and Conan-Guez (2006); Rossi and Villa (2006); Laloë (2008).  
890 Under assumption (A1), by Theorem 1 and with an argument similar to  
891 those developed in the proof of Corollary 1,  $\sigma(\hat{X}_{\lambda_d, \tau_d}) = \sigma(\{X(t)\}_{t \in \tau_d})$ .  
892 From assumption (A4b),  $\sigma(\{X(t)\}_{t \in \tau_d})$  is clearly a filtration. More-  
893 over, as  $\mathbb{E}(Y)$  and thus  $\mathbb{E}(Y^2)$  are finite,  $\mathbb{E}(Y|\hat{X}_{\lambda_d, \tau_d})$  is a uniformly  
894 bounded martingale for this filtration (see Lemma 35 of Pollard (2002)).  
895 This martingale converges in  $L^1$ -norm to  $\mathbb{E}(Y|\sigma(\cup_d \sigma(\hat{X}_{\lambda_d, \tau_d})))$ ; we  
896 have

- 897 •  $\sigma(\cup_d \sigma(\hat{X}_{\lambda_d, \tau_d})) \subset \sigma(X)$  as  $\hat{X}_{\lambda_d, \tau_d}$  is a function of  $X$  (via Theo-
- 898 rem 1);
- 899 • by Theorem 2,  $\hat{X}_{\lambda_d, \tau_d} \xrightarrow{d \rightarrow +\infty, \text{ surely}} X$  in  $L^2$  which proves that  $X$
- 900 is  $\sigma(\cup_d \sigma(\hat{X}_{\lambda_d, \tau_d}))$ -measurable.

901 Finally,  $\mathbb{E}(Y|\sigma(\cup_d \sigma(\hat{X}_{\lambda_d, \tau_d}))) = \mathbb{E}(Y|X)$  and  
902  $\mathbb{E}(Y|\hat{X}_{\lambda_d, \tau_d}) \xrightarrow{d \rightarrow +\infty, L^1} \mathbb{E}(Y|X)$ .

903 The conclusion follows from the fact that:

- 904 (a) *binary classification case*: the bound  $L_d^* - L^* \leq$   
 905  $2\mathbb{E} \left( \left| \mathbb{E} \left( Y | \hat{X}_{\lambda_d, \tau_d} \right) - \mathbb{E} (Y | X) \right| \right)$  (see Theorem 2.2 of  
 906 Devroye et al. (1996)) concludes the proof;
- 907 (b) *regression case*: as  $\mathbb{E}(Y^2)$  is finite,  $\mathbb{E} \left( \mathbb{E} \left( Y | \hat{X}_{\lambda_d, \tau_d} \right)^2 \right)$  is also fi-  
 908 nite and the convergence also happens for the quadratic norm (see  
 909 Corollary 6.22 in Kallenberg (1997)), i.e.,

$$\lim_{d \rightarrow +\infty} \mathbb{E} \left( \left( \mathbb{E} (Y | X) - \mathbb{E} \left( Y | \hat{X}_{\lambda_d, \tau_d} \right) \right)^2 \right) = 0$$

910 Hence, as  $L_d^* - L^* = \mathbb{E} \left( \left( \mathbb{E} (Y | X) - \mathbb{E} \left( Y | \hat{X}_{\lambda_d, \tau_d} \right) \right)^2 \right)$ , the con-  
 911 clusion follows.

#### 912 9.4. Theorem 3

913 We have

$$L(\phi_{n,d}) - L^* = L\phi_{n,\tau_d} - L_d^* + L_d^* - L^*. \quad (12)$$

914 Let  $\epsilon$  be a positive real. By Corollary 3, it exists  $d_0 \in \mathbb{N}^*$  such that, for all  
 915  $d \geq d_0$ ,

$$L_d^* - L^* \leq \epsilon. \quad (13)$$

916 Moreover, as shown in Corollary 1 and as  $\mathbf{Q}_{\lambda_d, \tau_d}$  is invertible, we have  
 917 in the binary classification case:  $L_d^* = \inf_{\phi: \mathbb{R}^{|\tau_d|} \rightarrow \{-1,1\}} \mathbb{P}(\phi(\mathbf{X}^{\tau_d}) \neq Y) =$   
 918  $\inf_{\phi: \mathbb{R}^{|\tau_d|} \rightarrow \{-1,1\}} \mathbb{P}(\phi(\mathbf{Q}_{\lambda_d, \tau_d} \mathbf{X}^{\tau_d}) \neq Y)$ , and in the regression case:  $L_d^* =$   
 919  $\inf_{\phi: \mathbb{R}^{|\tau_d|} \rightarrow \mathbb{R}} \mathbb{E}([\phi(\mathbf{X}^{\tau_d}) - Y]^2) = \inf_{\phi: \mathbb{R}^{|\tau_d|} \rightarrow \mathbb{R}} \mathbb{E}([\phi(\mathbf{Q}_{\lambda_d, \tau_d} \mathbf{X}^{\tau_d}) - Y]^2)$ . By hy-  
 920 pothesis, for any fixed  $d$ ,  $\phi_{n,\tau_d}$  is consistent, that is

$$\lim_{n \rightarrow +\infty} \mathbb{E}(L(\phi_{n,\tau_d})) = \inf_{\phi: \mathbb{R}^{|\tau_d|} \rightarrow \{-1,1\}} \mathbb{P}(\phi(\mathbf{Q}_{\lambda_d, \tau_d} \mathbf{X}^{\tau_d}) \neq Y),$$

921 in the classification case and

$$\lim_{n \rightarrow +\infty} \mathbb{E}(L(\phi_{n,\tau_d})) = \inf_{\phi: \mathbb{R}^{|\tau_d|} \rightarrow \mathbb{R}} \mathbb{E}([\phi(\mathbf{Q}_{\lambda_d, \tau_d} \mathbf{X}^{\tau_d}) - Y]^2),$$

922 in the regression case, and therefore for any fixed  $d_0$ ,  
 923  $\lim_{n \rightarrow +\infty} \mathbb{E}(L(\phi_{n,\tau_{d_0}})) = L_{d_0}^*$ . Combined with equations (12) and  
 924 (13), this concludes the proof.